

1                   **Assessing the Sensitivity of Local Snow Cover to Global Climate Change:**  
2                   **A General Method and Its Application to Five Swiss Locations**

3  
4                   Dimitrios Gyalistras<sup>1</sup>, Mario B. Rohrer<sup>2</sup>, Christoph Wahrenberger<sup>2</sup>,  
5                   Daniela Lorenzi<sup>2</sup> & Manfred Schwarb<sup>1,2</sup>

6                   *Manuscript submitted to Climate Dynamics*<sup>3</sup>

7                   9. May 2005

8                   **Abstract**

9                   A general method to assess possible changes in local snow cover statistics due to global  
10                  climate change was tested and applied at five representative Swiss sites located between  
11                  1018 and 2540 m. The method combines spatial and temporal downscaling of General  
12                  Circulation Model (GCM) outputs to the local and hourly space and time scales with a  
13                  conceptual snow model. Extensive validation experiments showed that the temporal  
14                  downscaling procedure can be used to accurately reproduce seasonal to decadal variations  
15                  of the local snow cover based on only 8 monthly input variables related to temperature (T)  
16                  and precipitation (P). The climatic sensitivity of several snow depth statistics was  
17                  studied for various combinations of changes in long-term mean T and P, plus two GCM-  
18                  downscaled climate change scenarios. All simulations showed a general decrease in snow  
19                  cover. In agreement with observations and earlier modelling studies the highest sensitivities  
20                  were obtained at the sites  $\leq 1600$  m and for the melting period in spring. The obtained  
21                  results can be explained by (i) the dominating, negative effect of a warming in situations  
22                  where present-day T is close to the freezing point; (ii) the generally negative effect of a  
23                  decrease in P; and (iii) the increasingly positive effect of an increase in P with decreasing T  
24                  below the freezing point. It was found that at elevations above ca. 2500 m an increase in  
25                  winter mean P by 20% could offset the effects of a 4 °C warming, at least for the time  
26                  from October through March. The long-term mean numbers of days with snow depths  
27                  above 0, 30 and 50 cm were found to decrease by on average 17, 14 and 11 days per °C  
28                  increase in November-April mean T. The relative frequencies of years with snow depth  
29                  exceeding 0, 30 and 50 cm for at least 100 days during the main skiing season were found  
30                  to decrease by on average 19%, 12% and 9% per °C. The proposed method was found to  
31                  be flexible, more accurate than similar alternative methods, and capable of providing  
32                  robust, physically plausible scenarios for possible changes in future snow cover.

---

<sup>1</sup> Climatology and Meteorology, Institute of Geography, University of Berne, Hallerstr. 12, CH-3012 Berne, Switzerland. Phone: +41 (0)78 / 602 54 09; e-mail: gyalistras@climate-impacts.ch

<sup>2</sup> Meteodat GmbH, Technoparkstr. 1, CH-8005 Zurich, Switzerland.

<sup>3</sup> Manuscript available electronically under <http://www.climate-impacts.ch/DGGreyLit.html#41>.

## 1. INTRODUCTION

Snow is an important feature of the physical environment of mid-latitude mountain regions such as the European Alps. It affects the climate system by modulating the fluxes of energy and water, it influences the dynamics of glaciers, permafrost and debris, and it is important for the ecology of many plant and animal species. With regard to human activities it affects among other things agriculture, water supply and hydroelectric energy production; it causes avalanches that may endanger humans, settlements and infrastructure; and it presents a major resource for the winter tourism industry by enhancing the aesthetic value of the landscape and providing the basis for many winter sports.

The anticipated changes in the Earth's climate (CUBASCH et al. 2001) are likely to have a strong impact also on the Alpine snow cover. The impact will depend on changes in the large-scale climate forcing (e.g., WANNER et al. 2000, SCHERRER et al. 2004), as well as on possible changes in regional-scale climate processes and feedbacks (e.g., FÖHN 1990, GIORGI et al. 1997). The analysis by LATERNSEER & SCHNEEBELI (2003) suggests that snow cover in Switzerland is already reacting to the observed 20th century warming.

Clearly, any further changes in the availability and space-time distribution of snow will have numerous implications and deserve closer consideration. The future development of the Alpine snow cover depends however on basic unknowns, such as the future radiative forcing of the global climate system. Planning for an uncertain future can be based on two major approaches: First, on the assessment of the snow cover's climatic sensitivity, understood as the system's response to unit changes in the statistics of driving weather variables. Second, on the construction of quantitative snow cover scenarios. Scenarios are no predictions, but rather consistent descriptions of possible futures that could occur if particular key assumptions, such as specific changes in global and regional climate patterns, would become true.

Sensitivities and scenarios for the snow cover in the European Alps have been studied based on climatological reasoning (FÖHN 1990), statistical analyses of observations (KOCH & RUDEL 1990, BREILING & CHARAMZA 1999, HANTEL et al. 2000, BENISTON et al. 2003a, WIELKE et al. 2004), and simulation models (BULTOT et al. 1992 and 1994, BRAUN et al. 1994, BAUMGARTNER & RANGO 1995, SCHULLA 1997, MARTIN et al. 1997, EHRLER 1998, STADLER et al. 1998, BENISTON et al. 2003b, JASPER et al. 2004). These studies suggested a high sensitivity of the Alpine snow cover to warming; they generally identified the largest sensitivities at elevations below 1500-2000 m, and in the spring season; and they provided some quantitative estimates of possible future changes in the region's snow climatology. However, several problems and open questions still remain:

First, most of the above studies have attempted to quantify possible changes but for a few selected snow cover statistics, such as the average length of the period with snow lying on the ground, or the annual mean water equivalent or depth of the snow cover. Exceptions are the studies by BULTOT et al. (1994) and SCHULLA (1997) that provided some information on possible changes in the numbers of days during the main skiing season (December to April) where snow depth exceeds a given threshold (e.g., 30 cm).

75 Second, most existing studies have considered only possible changes in long-term mean  
76 conditions. However, for many applications possible changes in the seasonal, interannual,  
77 or decadal-scale variability of the snow cover are considered to be at least as important as  
78 changes in the mean. For instance, ABEGG (1996) and BÜRKI (2000) argue that the winter  
79 tourism industry depends more sensitively on the frequency and regularity of "good" and  
80 "bad" years for skiing than on long-term average conditions.

81 Third, most studies have investigated but a limited range of possible future changes in  
82 climate. An exception is the study by JASPER et al (2004) that considered 23 different  
83 climate change scenarios. Although this work dealt only marginally with snow cover it  
84 clearly suggested a high sensitivity of the projected changes to the choice of climate change  
85 scenario. A similar result was reported by MARTIN et al. (1997). On the other hand,  
86 STADLER et al. (1998) reported very similar snow cover responses to two strongly  
87 differing climate change scenarios. To our knowledge, the role of uncertainty in the driving  
88 climate scenarios has not been investigated in much detail to date.

89 Finally, a basic problem occurs due to conflicting requirements related to the physical  
90 consistency, robustness and spatio-temporal resolution that can be attained in sensitivity  
91 or scenario studies. Statistical models that link observed spatial or temporal climate  
92 variations to variations of the snow cover can be considered very robust if they have be  
93 based on a large data base that covers a wide range of situations (e.g., HANTEL et al. 2000).  
94 However, such models can only be expected to accurately predict averages over larger  
95 areas and/or longer time periods, at best, and this contrasts with the needs of many  
96 applications. Very detailed information can in principle be obtained from simulations with  
97 dynamic snow models that may include very sophisticated representations of snow  
98 physics and radiation processes (e.g., ETCHEVERS et al. 2004). Simulation studies are  
99 however typically limited by their demanding needs for meteorological input data at a  
100 daily or even hourly time step. Moreover, the question arises how the high-frequent  
101 weather variability should be included in the driving weather scenarios, and how this  
102 variability affects the robustness of the resulting projections.

103 In this work we address the above problems by presenting, testing and applying a new  
104 method that is intermediate between the statistical and physically-based modelling  
105 approaches. The method requires only monthly weather data as an input, but we show  
106 that it is able to provide physically plausible and robust snow cover scenarios at high  
107 spatial and temporal resolutions. As a case study we consider the snow needs of the  
108 winter tourism industry at five representative Swiss locations. We explore a wide range of  
109 possible changes in key temperature and precipitation parameters, including two regional  
110 climate change scenarios that were derived from simulations with two global climate  
111 models. We use two older climate model runs, mainly for illustrative purposes. The focus  
112 of our study lies in the presentation of the new method and the analysis of the climatic  
113 sensitivity of the Swiss snow cover.

114 In the next section we describe our method and the datasets and models used. Section 3  
115 presents the results of our simulations and compares them to findings from earlier studies.  
116 Section 4 provides a discussion of the found sensitivities and of the proposed method. The  
117 conclusions of our study are given in Section 5.

## 2. DATA & METHODS

### 2.1 Overview

Fig. 1 gives an overview of the proposed method. It employs an array of models and has two main inputs: possible future changes in global radiative forcing agents (Fig. 1, top left), and the needs of impact analysts for snow cover scenarios (bottom right). The main output is given by changes in selected local snow cover statistics (top right). Additional inputs are given by various large-scale and local measurements that are used to calibrate the individual models (Fig. 1, bottom).

The design of our method was based on a series of general considerations that have been discussed in detail by GYALISTRAS et al. (1997) and GYALISTRAS & FISCHLIN (1999). Therefore, here we give only a brief outline of the design rationale. The implementation of the individual steps is presented in more detail in the following subsections. Possible limitations of the method and alternative approaches are discussed later in Section 4.

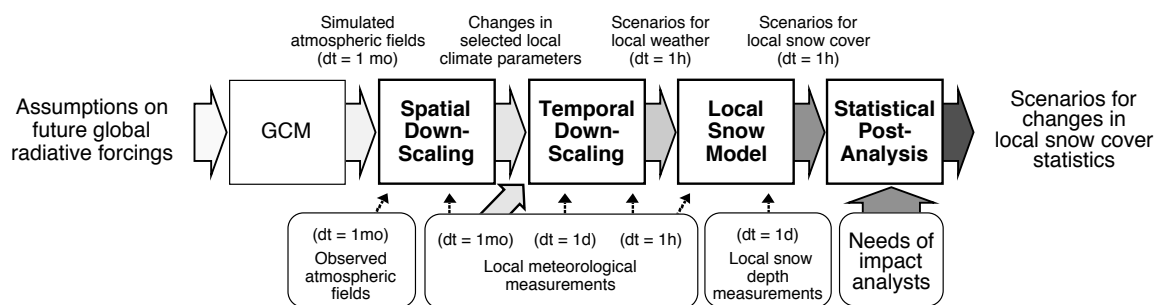


**Figure 1:** Overview of the procedure used to assess the sensitivity of the local snow cover and to project future scenarios. GCM: General Circulation Climate Model. Arrows: flow of information; top: major procedures/models; bottom: auxiliary data used to determine model parameters; dt = time step.

Following a fairly standard approach to climate scenario construction (MEARNS et al. 2001) the first step of our procedure consists in making available results from scenario runs with General Circulation Climate Models ("GCM", see Fig. 1). The second step deals with the problem that GCMs have a coarse horizontal resolution and thus show only limited skill at spatial scales below several hundreds of km (e.g. VON STORCH, 1995, WIDMANN & BRETHERTON 2000). Therefore a statistical procedure is employed to estimate possible shifts in local climate parameters as a function of the large-scale climatic changes simulated by a given GCM simulation ("Spatial Downscaling"). The third step serves the generation of hourly weather sequences consistent with a given set of present-day or hypothetical future climatic conditions ("Temporal Downscaling"). This step is accomplished with the aid of a stochastic weather generator that is forced by present-day ("control" case) or appropriately perturbed ("scenario" case) monthly weather data. In a fourth step the synthetic hourly weather sequences are used to drive a dynamic simulation model of snow water equivalent and snow depth ("Local Snow Model"). The snow model's results are finally analyzed to derive various statistics, e.g. as required by our winter tourism case study ("Statistical Post-Analysis").



152

153

154

**Figure 2:** Relief map of Switzerland and location of the five case study sites. Copyright for the relief map by "K606-01©2004 swisstopo".

155

**Table 1:** Overview of the case study sites and their climatic conditions

Site	Location	Elevation (m)	$T_{win}$ (°C)	$P_{win}$ (mm)	$P_{probwin}$ (-)	$N_d(S > 0)$ (-)
Engelberg	Valley floor, Northern Alps	1018	0.7	624	0.52	123
Disentis	Valley floor, Central Alps	1190	1.0	445	0.44	129
Montana	South-facing slope, Central Alps	1495	0.3	575	0.41	139
Davos	Valley floor, Central Alps	1590	-2.2	372	0.42	164
Weissfluhjoch	Mountain peak, Central Alps	2540	-7.1	542	0.53	180

156

157

158

159

$T_{win}$ ,  $P_{win}$ ,  $P_{probwin}$ : winter half-year (November-April) mean temperature, total precipitation and average monthly precipitation probability; shown are long-term mean values for the period 1971-1995.  $N_d(S > 0)$ : long-term mean number of days at which snow depth  $S$  exceeds 0 cm in the period Nov. 1 - Apr. 30, winters 1971/72 - 1994/95.

160

161

162

163

164

The method was applied to 5 Swiss sites (Fig. 2) that were located at an elevation range between 1018 and 2540 m (Table 1). We chose these sites because of the availability of high-quality, long-term snow data (see below), because they represent the most important climatic regions of the Swiss Alps, and because of their vicinity to important ski tourism destinations.

165

## 2.2 Data

166

### 2.2.1 Large-scale Data

167

168

169

The fitting of the spatial downscaling models required large-scale (predictors) and local (predictands) weather data. The predictors were given by gridded anomaly fields for monthly mean sea-level pressure (SLP) and monthly mean near-surface temperature

170 (NST). Both fields had a 5° x 5° latitude/longitude resolution and were defined over the  
171 sector 40°E-40°W and 30°N-70°N. We used data for the years 1931-1980, and the  
172 anomalies were defined relative to the long-term mean of this period. The SLP data were  
173 those by TRENBERTH & PAOLINO (1980). For NST we used the data set by JONES &  
174 BRIFFA (1992) and BRIFFA & JONES (1993). A newer data set would have been available  
175 for NST, but for the sector and period considered it would probably differ only little from  
176 the one used here (see JONES & MOBERG 2003).

177 For the generation of the local climate change scenarios we considered simulations with  
178 two GCMs, the ECHAM1/LSG model of the Max Planck Institute for Meteorology,  
179 Hamburg, and the GCMII model of the Canadian Climate Centre (CCC), respectively.  
180 The large-scale SLP and NST input fields to the spatial downscaling procedure were  
181 determined as follows: For the ECHAM model we used anomalies from a 100 year  
182 "2xCO<sub>2</sub>" (720 ppmv) simulation relative to the 40-year mean of a "1xCO<sub>2</sub>" (344 ppmv)  
183 simulation (CUBASCH et al. 1992). For the CCC model we used anomalies for 5 simulated  
184 years under 660 ppmv (BOER et al. 1992) relative to the mean from 5 years under 330  
185 ppmv (MCFARLANE et al. 1992).

186 Newer GCM simulations (see CUBASCH et al. 2001 for an overview) would have been  
187 available for the present study. We chose to use these older runs for several reasons.  
188 Firstly, we wanted our snow cover scenarios to be consistent with earlier Swiss studies  
189 that have investigated climatic impacts on grasslands (RIEDO et al. 1997, 1999), forests  
190 (FISCHLIN & GYALISTRAS 1997) and hydrology (SCHULLA 1997, STADLER et al. 1998)  
191 using the same GCM simulations. Secondly, we wanted to profit from earlier experience  
192 (GYALISTRAS et al. 1994, 1997, 1998) with the two GCMs. Third, as is shown later  
193 (Section 3), the two sets of downscaled scenarios showed some interesting differences.  
194 Finally, these older GCM runs sufficed for our purposes, since we were mainly interested  
195 in method development and the exploration of sensitivities rather than in deriving the  
196 "best" currently possible projections for future snow cover.

### 197 **2.2.2 Local Data**

198 Long-term ( $\geq 25$  years) time series of monthly weather statistics up to the year 1995 were  
199 used at the five case study sites in order to fit the spatial downscaling models, to  
200 interpolate climate change scenarios across sites, and to drive the temporal downscaling  
201 procedure. All needed monthly weather data were derived from daily local temperature  
202 and precipitation measurements that were extracted from the "KLIMA" data base of the  
203 Swiss Federal Office for Meteorology (MeteoSwiss).

204 Spatial downscaling was applied to 22 monthly weather statistics related to temperature  
205 (T), precipitation (P), global radiation (GR), vapour pressure (VP) and wind speed (WS)  
206 (see GYALISTRAS et al. 1997). However, only the following 8 variables mattered for the  
207 snow simulations and will be addressed in more detail in the present study: the monthly  
208 total P, the monthly P probability (Pprob; estimated by the relative frequency of the days  
209 with daily precipitation  $\geq 1$  mm), and the monthly mean and within-month standard  
210 deviation of daily mean, minimum and maximum T.

211 For the fitting of the temporal downscaling procedure we used at each site 5 years (1981-  
212 1985) of daily and hourly data, which were extracted from the "ANETZ" database of  
213 MeteoSwiss. Details on the data preparation can be found in GYALISTRAS et al. (1997).

214 At all 5 case study locations we used 14 years of daily snow depth data to tune the snow  
215 model and up to 50 years of additional daily data to test the temporal downscaling/snow  
216 model chain. Snow data were taken from the snow database of the Hydrology section of  
217 the Institute of Geography, ETH Zurich (ROHRER 1992) and from the snow depth  
218 database of MeteoSwiss (WITMER 1986). The snow data were quality checked and  
219 cleaned for errors and missing data as described in the above mentioned monographs.

## 220 **2.3 Spatial Downscaling**

221 Spatial downscaling was based on the method of GYALISTRAS et al. (1994). According to  
222 this method we first established multivariate regression models that linked interannual  
223 variations of the 22 local monthly weather statistics to simultaneous anomalies of the  
224 monthly SLP and NST fields. The use of additional predictor fields related to atmospheric  
225 humidity would have been desirable (e.g. CHARLES et al. 1999, BECKMANN & BUIHAND  
226 2002). However, this was not possible because no corresponding GCM data were  
227 available as an input for scenario construction.

228 The regression models were determined from a Canonical Correlation Analysis (CCA, e.g.  
229 VON STORCH & ZWIERS 1999) in the space spanned by the first few Empirical Orthogonal  
230 Functions (EOFs) of the predictor and predictand variables. We performed CCA for the  
231 period 1931-1980 separately for each month and for each of the 3 sites Davos, Montana  
232 and Engelberg.

233 Since CCA is known to depend quite sensitively on the choice of the numbers of used  
234 predictor and predictand EOFs we performed for each month and location several CCAs  
235 using the first 4 to 10 predictor EOFs and the first 5 to 8 predictand EOFs. These  
236 numbers were determined based on a systematic investigation of CCA models that used  
237 different numbers of EOFs. The lower numbers were given by the numbers of EOFs at  
238 which the found correlations between the predictor and predictand data sets started to  
239 level off. The upper numbers were given by the numbers of EOFs that were typically  
240 needed to explain ~90% of the total variance in the respective data sets.

241 In a second step we estimated possible future changes in the local weather statistics by  
242 applying the regression models to the GCM-simulated anomaly fields (see previous  
243 section). For the predictions we considered for each individual CCA model all canonical  
244 modes that showed a squared canonical correlation coefficient  $\geq 0.15$ .

245 The downscaled climate change scenarios were given by site-specific changes in the long-  
246 term mean annual cycles of the monthly weather statistics. The changes were estimated  
247 by averaging the downscaled weather anomalies from 100 (ECHAM) or 5 (CCC) years  
248 and from all fitted 28 CCA models per site and month. The downscaled signals showed  
249 rather jagged annual cycles which were smoothed by assigning to each month the 0.25-1-  
250 0.25 weighted average value of the downscaled anomalies from that month and the two  
251 neighbouring months.

252 Due to the lack of long-term local measurements, the spatial downscaling procedure could  
253 not be applied to the sites Disentis and Weissfluhjoch. Climate change scenarios at these  
254 sites were obtained by interpolating the downscaled changes from the site Davos, which is  
255 located at a distance of 77 km from Disentis and ~3 km from Weissfluhjoch, respectively  
256 (Fig. 2). Interpolation was done with the aid of linear regression models which were fitted

257 separately for each weather statistic and month. To this purpose we used data for the  
258 years 1961-1996 for Disentis and 1971-1996 for Weissfluhjoch.

## 259 **2.4 Temporal Downscaling**

260 For temporal downscaling we used the method of GYALISTRAS et al. (1997; see also  
261 GYALISTRAS & FISCHLIN 1999). The method was implemented with the aid of the local  
262 stochastic weather generator WeathGen (version 2.5b). WeathGen simulates hourly  
263 weather data conditional on monthly weather inputs in two steps: the first step serves the  
264 transition from monthly to daily weather, the second step the transition from daily to  
265 hourly weather. A simulated hourly weather sequence is fully determined by (i) the  
266 parameters of the assumed stochastic processes (see below); (ii) the monthly weather  
267 inputs; and (iii) the initialization of the random number generator incorporated in  
268 WeathGen.

269 The monthly weather was described by 22 variables (monthly total P, Pprob, and the  
270 monthly means and within-month standard deviations of GR, and daily mean, minimum  
271 and maximum T, VP and WS), the daily weather was described by 11 variables (daily total  
272 P, daily mean GR, and daily mean, minimum and maximum T, VP and WS), and the hourly  
273 weather by 5 variables (hourly total P and hourly mean GR, T, VP, and WS). For  
274 technical reasons we applied temporal downscaling to all above weather variables, but  
275 actually only the generated hourly P and T values were used to drive the snow model.

276 Both transitions, from monthly to daily and from daily to hourly weather, are  
277 accomplished in WeathGen based on first-order Markov chain-exponential models to  
278 simulate P and first-order auto-regressive models to simulate all other variables conditional  
279 on P. To ensure consistency among temporal aggregation levels, WeathGen repeatedly  
280 simulates daily (or hourly) weather sequences until the statistics of a simulated sequence  
281 for a given month (day) are sufficiently close to the respective monthly (daily) inputs.  
282 Once a weather sequence has been accepted it is adjusted such, that its statistics exactly  
283 reproduce the prescribed inputs (GYALISTRAS et al. 1997).

284 WeathGen requires a large number of site- and month-specific stochastic process  
285 parameters which were determined separately for each site for the years 1981-1985 and  
286 were left unchanged in all simulations. In order to simulate hourly weather data under  
287 historical and changed climatic conditions we only perturbed the monthly inputs, as  
288 described in Section 2.8.

## 289 **2.5 Snow Model**

290 The used snow model was based on the model by BRAUN & RENNER (1992) that was  
291 adapted to simulate local snow cover at a hourly time step. We chose this higher temporal  
292 resolution in order to be able to discriminate more accurately between rain and snow in the  
293 simulations.

294 The modified model requires hourly T and P as inputs and produces the following  
295 outputs: hourly values for the total water equivalent of the snow cover (W, in mm), plus  
296 snow depth (S, in cm) at 07.00 UTC. The model operates at two time steps, an hourly  
297 time step, with index k, and a daily time step, with index  $q = \text{DIV}(k-1, 24) + 1$ , where

298 DIV(x, y) denotes the integer division of x by y. The value range of the indices is  $1 \leq q \leq$   
 299  $q_{\max}$  and  $1 \leq k \leq 24 * q_{\max}$  with  $q_{\max} \leq 335$  (cf. Table 3).

300 The hourly ( $W_H$ ) and daily ( $W_D$ ) values for W were calculated according to

$$301 \quad W_{H(k)} = W_{s(k)} + W_{l(k)} \quad (\text{Eq. 1a})$$

$$302 \quad W_{D(q)} = W_{H(24(q-1)+1)} \quad (\text{Eq. 1b})$$

303 where  $W_s$  and  $W_l$  are the solid (snow plus ice) and the liquid water content of the snow  
 304 cover, respectively (both in mm). These two variables are updated according to:

$$305 \quad W_{s(k+1)} = \text{MAX}(0, W_{s(k)} - A(k) + F(k) + P_s(k)) \quad (\text{Eq. 2a})$$

$$306 \quad W_{l(k+1)} = \text{LIM}(0, W_{\max(k+1)}, W_{l(k)} + A(k) - F(k) + P_l(k)) \quad (\text{Eq. 2b})$$

307 Here A denotes the ablation of the snow cover, F the amount of re-frozen meltwater,  $P_s$   
 308 the hourly total solid precipitation,  $W_{\max}$  the maximum water holding capacity of the  
 309 snow cover, and  $P_l$  the hourly total liquid precipitation (all variables in mm);  $\text{MAX}(x, y)$   
 310 is a function that returns the maximum of x and y; and  $\text{LIM}(x, y, z)$  is a function that  
 311 limits the value of z to between x and y.

312 The melting of snow (quantity A) was modelled based on a degree day formula. Although  
 313 this formula is a rough approximation of the energy balance equation of the melting snow  
 314 cover, the resulting differences are usually quite small, as stated in WMO (1986). We  
 315 found that a seasonally varying degree day factor  $\alpha_{(d)}$  was best for the sites considered:

$$316 \quad A(k) = \text{MAX}(0, \alpha_{(q)} (T(k) - \tau_0) \Delta t) \quad (\text{Eq. 3a})$$

$$317 \quad \alpha_{(q)} = \alpha_{\min} + 0.5 (\alpha_{\max} - \alpha_{\min}) \left\{ 1 + \text{COS}\left(\frac{2\pi}{364} (q + \Delta q - 1)\right) \right\} \quad (\text{Eq. 3b})$$

318 T denotes the hourly mean air temperature (in °C),  $\tau_0$  the air temperature at which melting  
 319 starts (in °C; here 0 °C), and  $\Delta t$  the time increment per time step (1/24 d). The parameters  
 320  $\alpha_{\min}$  and  $\alpha_{\max}$  (Table 2) determine the seasonal extrema of  $\alpha$ , and  $\Delta q$  is the difference  
 321 between the day number of the first simulated day ( $q=1$ ) and the day number of the  
 322 summer solstice, which was always set to 172, i.e. the 21st of June.

323 Refreezing of meltwater in the snow cover was simulated as "negative melt" according to:

$$324 \quad F(k) = \text{MAX}(0, \phi (\tau_0 - T(k)) \Delta t) \quad (\text{Eq. 4})$$

325 where  $\tau_0$  and  $\Delta t$  are defined as above, and  $\phi$  is a site-specific parameter (Table 2).

326 The aggregational state of precipitation was determined using an air temperature divider  
 327  $\tau_{\text{crit}}$  (e.g., ROHRER 1989). To compensate for errors in precipitation measurements,  
 328 representativity of precipitation stations and interception losses, multiplicative correction  
 329 factors for solid (snowfall) and liquid (rainfall) precipitation were applied:

$$P_{s(k)} = \begin{cases} 0 & \text{if } T_{(k)} > \tau_{\text{crit}} \\ \kappa_s P_{(k)} & \text{if } T_{(k)} \leq \tau_{\text{crit}} \end{cases} \quad (\text{Eq. 5a})$$

$$P_{l(k)} = \begin{cases} \kappa_l P_{(k)} & \text{if } T_{(k)} > \tau_{\text{crit}} \\ 0 & \text{if } T_{(k)} \leq \tau_{\text{crit}} \end{cases} \quad (\text{Eq. 5b})$$

The used parameter values are given in Table 2.

The maximum water holding capacity of the snow cover was computed as

$$W_{\text{max}(k+1)} = \eta W_{s(k+1)} \quad (\text{Eq. 6})$$

where  $\eta$  is again a site-dependent parameter (Table 2).

In order to compute  $S$  the model traces the fate of  $i = 1..q_{\text{max}}$  individual snow layers at a daily time step. The water equivalents of the layers are converted to snow depths based upon a simple settling curve model developed by MARTINEC (1977) and further refined by ROHRER (1992). The layer depths ( $H_{i(q)}$ , in mm) are updated according to

$$H_{i(q)} = \begin{cases} H_{i0}(1+a)^{-\lambda} & \text{if } i \leq q \\ 0 & \text{if } i > q \end{cases} \quad (\text{Eq. 7a})$$

$$H_{i0} = \text{MAX}(0, \Delta W_i / \rho_o) \quad (\text{Eq. 7b})$$

Here the index  $i$  denotes the  $i$ -th layer, which comes into existence at day  $q = i$ , but actually matters only if net accumulation had taken place during the last 24 h (MAX function in Eq. 7b);  $a = q-i$  is the age of the snow in layer;  $H_{i0}$  is the layer's initial depth;  $\Delta W_i = W_{D(i)} - W_{D(i-1)}$  is the balance of  $W$  over the  $i$ -th simulated day; and  $\lambda$  and  $\rho_o$  are parameters (Table 2). The calibrated values for  $\rho_o$  were around  $100 \text{ kg m}^{-3}$  (Table 2), which compares well with measurements from the Swiss Alps (ROHRER et al. 1994).

The daily snow depth  $S$  (in cm) was finally computed based on the current density ( $D$ , in  $\text{kg m}^{-3}$ ) of the total snow pack according to

$$S_{(q)} = 100 W_{D(q)} / D_{(q)} \quad (\text{Eq. 8a})$$

$$D_{(q)} = \frac{\sum_{i=1}^q \rho_o H_{i0}}{\sum_{i=1}^q H_{i(q)}} \quad (\text{Eq. 8b})$$

The snow model was found to perform well if tested against independent observations (not shown), but if driven with temporally downscaled hourly data some systematic deviations were found. These were corrected empirically by fitting a scaling factor  $f$  according to

$$S'(q) = f S(q) \quad (\text{Eq. 9})$$

All results presented below actually refer to  $S'$ , but for the sake of simplicity we will address this variable from here on as  $S$ .

**Table 2:** Site-specific parameters of the snow model and fitted parameter values at the five case study sites

Symbol	Unit	Description	Engelberg	Disentis	Montana	Davos	Weiss-fluhjoch
$\alpha_{\min}$	mm °C <sup>-1</sup> d <sup>-1</sup>	Min. value of degree day factor (Dec. 21)	2.35	0.38	1.15	0.325	0.01
$\alpha_{\max}$	mm °C <sup>-1</sup> d <sup>-1</sup>	Max. value of degree day factor (June 21)	6.25	4.76	8.45	6.79	5.03
$\phi$	mm °C <sup>-1</sup> d <sup>-1</sup>	Coefficient of refreezing	2.38	2.09	4.31	2.55	2.32
F	--	Scaling factor for daily snow depths	1.00	1.25	1.24	1.21	1.23
$\eta$	--	Maximum rel. water holding capacity of snow	0.01	0.08	0.079	0.065	0.001
$\kappa_s$	--	Solid precipitation correction factor	1.88	1.18	1.46	1.235	1.25
$\kappa_l$	--	Liquid precipitation correction factor	0.64	1.26	0.74	0.69	0.854
$\lambda$	--	Exponential settling term of snow layer depth	0.37	0.38	0.325	0.32	0.3
$\rho_0$	kg m <sup>-3</sup>	Density of new-fallen snow	122	88	129	92	99
$\tau_{\text{crit}}$	°C	Threshold air temperature	0.41	0.1	0.7	0.2	-0.7

360

The site-specific parameter values (Table 2) were determined for the 14 winters 1981/82 to 1994/95 based on a comparison with measured daily data for  $S$ . This was done in two steps: First we drove the model using hourly measured weather data in order to tune all parameters except  $f$  (see Eq. 9). Initial parameter estimates were obtained by applying the automated algorithm of MONRO (1971) to data from the first 7 winters. Then we fine-tuned the parameters based on the remaining winters by visually comparing the simulated and observed  $S(q)$ . In a second step we drove the model with temporally downscaled monthly data and we determined  $f$  based on a visual comparison of the measured and simulated daily time series.

## 2.6 Statistical Post-Analysis

The following statistics of  $S$  were computed: (i) the long-term mean of  $S$  for every day of the year; (ii) the number of days ( $N_d$ ) within a given subperiod ( $P_i$ , see Table 3) of the winter season where  $S$  exceeds a given threshold ( $h$ ), denoted as  $N_d(S \geq h)$ ; and (iii) the relative frequency of years where  $N_d$  is below or above a given number of days ( $n_d$ ),  $\text{RF}[N_d < n_d]$  and  $\text{RF}[N_d \geq n_d]$ , respectively.

The used subperiods  $P_i$  are summarized in Table 3. Subperiod  $P_0$  presents the maximum period where persistent snow cover can be expected to occur at our case study sites. Subperiod  $P_1$  corresponds to the maximum period for which daily snow depth data were

379 available for model validation. Subperiods  $P_2$  and  $P_3$  were considered because of their  
380 relevance for winter tourism in Switzerland.

381 **Table 3:** Definition of the subperiods used to calculate snow depth statistics

Symbol	Description	Definition	Length (d)
$P_0$	Whole winter	Sep. 1 - Jul. 31	334
$P_1$	Winter half-year	Nov. 1 - Apr. 30	181
$P_2$	Main skiing season	Dec. 1 - Apr. 15	136
$P_3$	Christmas holiday	Dec. 20 - Dec. 31	12

382 Note: the lengths of the subperiods  $P_0$  to  $P_2$  refer to non leap years.

383 The snow depth thresholds considered were  $h = 0, 10, 20, 30, 40$  and  $50$  cm. We chose  
384 these values because depending on the terrain, typically at least  $10$  to  $20$  cm are needed for  
385 Nordic skiing and  $30$  to  $50$  cm for downhill skiing in the Swiss Alps.

386 The critical numbers of days  $n_d$  were chosen based on BÜRKI (2000) who drew upon  
387 earlier work by WITMER (1986) and ABEGG (1996). According to BÜRKI a "good" winter  
388 for downhill skiing is characterized by  $N_d \geq 100$  d during period  $P_2$ , whereas winters with  
389  $N_d < 40$  d must be considered as "bad" for the winter tourism industry. For subperiod  $P_3$   
390 we chose more or less arbitrarily  $n_d = 10$  d.

391 The absolute (AS) and relative (RS) sensitivities of a snow statistic  $X$  to a temperature  
392 increase were evaluated according to:

$$393 \quad AS = \partial X / \partial T_{win} \quad (Eq. 10)$$

$$394 \quad RS = AS / \bar{X} \quad (Eq. 11)$$

395 Here  $T_{win}$  is the winter half-year (November-April) long-term mean temperature, and  $\bar{X}$   
396 stands for the mean of all  $X$  values entering the analysis. The AS was estimated by the  
397 slope of the linear regression of  $X$  on  $T_{win}$ .

398 Note, RS differs from the relative change per degree warming ( $\Delta_{rel}$ ) that has been used in  
399 other studies. The latter is typically defined as  $\Delta_{rel} = ((X_{scen} - X_{ctrl}) / X_{ctrl}) / (T_{scen} - T_{ctrl})$   
400 where "ctrl" stands for present-day "control" and "scen" for "scenario" conditions. If only  
401 two data points are considered (e.g., one control and one scenario case) holds the  
402 relationship:

$$403 \quad RS = \Delta_{rel} / (1 + 0.5 \Delta_{rel}) \quad (Eq. 12)$$

404 We used RS instead of  $\Delta_{rel}$  because our aim was to estimate the average relative response  
405 of  $X$  in the vicinity of the working point  $(\bar{T}, \bar{X})$  based on many different value pairs  $(T,$   
406  $X)$ , rather than to describe relative departures from a particular starting point  $(T_{ctrl}, X_{ctrl})$ .  
407 For the comparison with other studies we therefore computed RS from the published  
408 results according to Eqs. 11 or 12.

409

## 2.7 Model Validation

410 The testing and validation of each single model involved in our procedure (Fig. 1) was  
411 beyond the scope of this work. The strengths and limitations of the two used GCMs have  
412 been addressed elsewhere (see GATES et al. 1996 for an overview, VON STORCH et al 1997  
413 for the ECHAM model, and MCFARLANE et al. 1992 for the CCC model).

414 The spatial downscaling procedure has been validated by GYALISTRAS et al. (1994, 1998)  
415 who found limited skill for some downscaled variables. Nevertheless, the procedure was  
416 found to yield for both GCMs physically plausible and spatially consistent changes in  
417 local climates, as discussed by FISCHLIN & GYALISTRAS (1997) and GYALISTRAS et al.  
418 (1997, 1998). The strengths and limitations of the regional climate scenarios are briefly  
419 discussed in Section 4.3.

420 In this work we focused on the validation of the temporal downscaling procedure in  
421 combination with the snow model since no such work has been reported so far. The test  
422 setup was as follows: the temporal downscaling/snow model chain was driven with  
423 measured monthly weather data and the simulated snow depth statistics were then  
424 compared with corresponding statistics that were derived from the daily snow  
425 measurements.

426 The comparison was based on independent data from the following winters: 1970/71-  
427 1980/81 for Engelberg (n=11), 1961/62-1980/81 for Disentis (n=20), 1951/52-1980/81 for  
428 Montana (n=30), 1930/31-1980/81 for Davos (n=51), and 1971/72-1980/81 for  
429 Weissfluhjoch (n=10).

430

## 2.8 Simulation Experiments

431 In order to be consistent with the snow depth measurements all simulations started at  
432 07.00 UTC on the first day of period  $P_0$  (Table 3). The state variables  $W_s$ ,  $W_l$  and  $H_l$  were  
433 initialized at the beginning of the first hour ( $k=q=0$ ) of each simulated winter to zero, i.e.  
434 the individual winters were simulated independently from each other.

435 Since the temporal downscaling procedure incorporates a stochastic component we ran the  
436 snow model at least  $n_{\text{realiz}} = 30$  times per winter, using the same monthly input data but  
437 different initial values for the random number generator within WeathGen. We then  
438 analyzed the simulated snow depth data separately for each run and determined the final  
439 snow cover statistics by taking averages over the statistics from all runs per winter. The  
440 number of 30 realizations was chosen because it was found that from this sample size on  
441 the multi-run statistics typically did not change by more than a few percents if an  
442 additional realization of the hourly weather was considered. For model validation we used  
443 throughout  $n_{\text{realiz}} = 30$ .

444 For the sensitivity and scenario experiments we used monthly input data from the  
445 following winters: 1971/72 - 1994/95 for Engelberg (n=24), 1961/62 - 1994/95 for  
446 Disentis (n=34), 1931/32 - 1994/95 for Montana (n=64), 1901/02-1993/94 for Davos  
447 (n=93), and 1971/72 - 1994/95 for Weissfluhjoch (n=24).

448 In order to be able to compare the results between sites, changes in the long-term mean  
449  $N_d(S \geq h)$  were evaluated using only the common subset of winters 1981/82-1994/95 ( $n =$

450 14). This is not a very large sample, but note that these winters covered a wide range of  
451 conditions with abundant snow at the beginning of the 1980s and very little snow in the  
452 winters 1987/88 to 1989/90. Moreover, in order to enhance the statistical robustness of  
453 our results, in this case we used  $n_{\text{realiz}} = 100$ . For the RF statistics, which depended on  
454 annual snow cover indices, we considered all winters for which input data were available  
455 and we used  $n_{\text{realiz}} = 30$ .

456 The effects of a given climatic change scenario were simulated by shifting each element of  
457 the monthly time series that were used to drive the temporal downscaling procedure by  
458 the same scenario-, month- and location-specific amount. The year-to-year variability of  
459 the monthly time series was always left unchanged.

460 For the systematic study of sensitivities we considered 4 synthetic scenarios which  
461 specified seasonally uniform changes by +2 and +4 °C for T and by  $\pm 20\%$  for P. These  
462 scenarios were named T2Pp, T2Pm, T4Pp and T4Pm, where "p" and "m" stand for plus  
463 and minus 20%, respectively. The 8 relevant monthly input variables for the snow  
464 simulations were adjusted in these scenarios as follows: the same T increase was applied  
465 to the monthly means of daily mean, minimum and maximum T; the within-month  
466 standard deviations of the daily T variables were left unchanged; and the assumed change  
467 in P was associated with a change of the same sign in Pprob by 10%.

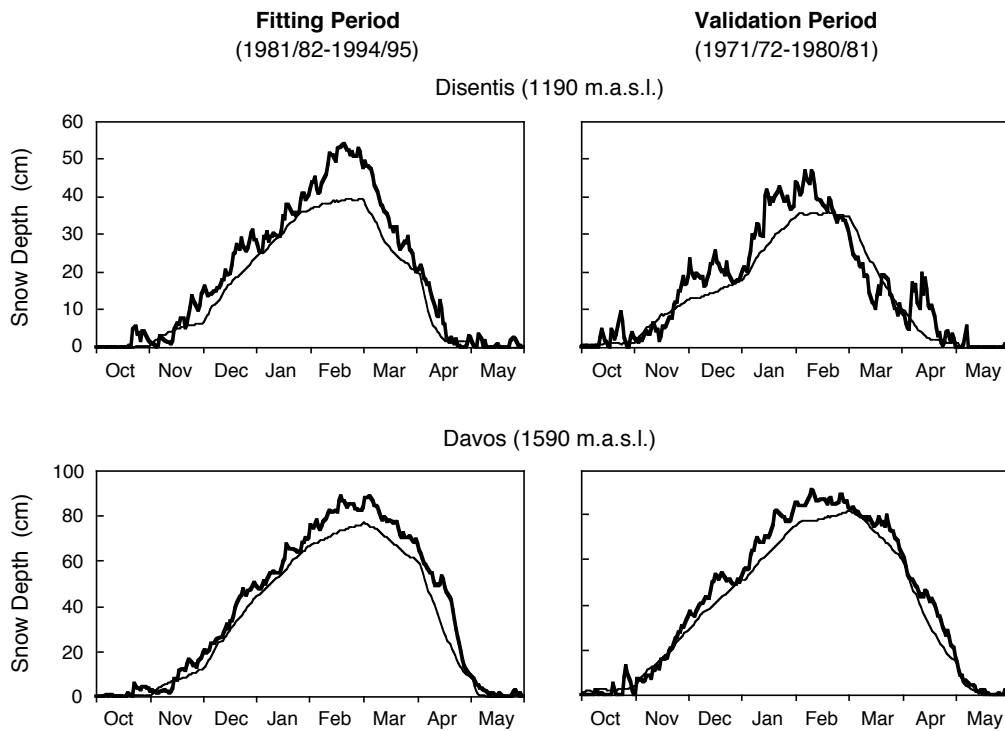
468 The ECHAM and CCC scenarios specified changes not only for the monthly means, but  
469 also for the within-month standard deviations of the T variables (see Section 2.2). The  
470 two GCM-based scenarios are presented in more detail in Section 3.2. In order to study  
471 the effects of a gradual shift in climate we formulated additional scenarios by scaling all  
472 originally downscaled changes by a factor  $s$  varying from 0.2 to 2.0 in steps of 0.2. An  
473 exception was applied to the within-month standard deviations of daily mean, minimum  
474 and maximum T under the CCC scenario. The changes for these three variables were found  
475 to be quite large (see later), and in order to restrict them to a plausible value range they  
476 were scaled only up to  $s = 1.0$  and then they were kept constant to the originally  
477 downscaled values. The resulting scenarios were named ECH-TR( $s$ ) and CCC-TR( $s$ ),  
478 where TR stands for transient climate change.

## 479 3. RESULTS

### 480 3.1 Validation of the Temporal Downscaling/Snow Model Chain

481 Fig. 3 shows the measured and simulated long-term mean S at the sites Disentis and  
482 Davos. It can be seen that the seasonal development of S was reproduced in the validation  
483 period as well as in the fitting period. The simulations yielded a much smoother seasonal  
484 cycle than the measurements and tended somewhat to underestimate S. This tendency  
485 was smaller at the lowest site, Engelberg, and more pronounced at the highest site,  
486 Weissfluhjoch (not shown).

487 Fig. 4 compares the observed and simulated numbers of days at which S exceeds the 30 cm  
488 threshold in period P<sub>1</sub>, again using the sites Disentis and Davos as an example. It can be  
489 seen that the simulations captured the observed interannual to decadal-scale variability of  
490 the S statistics with very good skill.

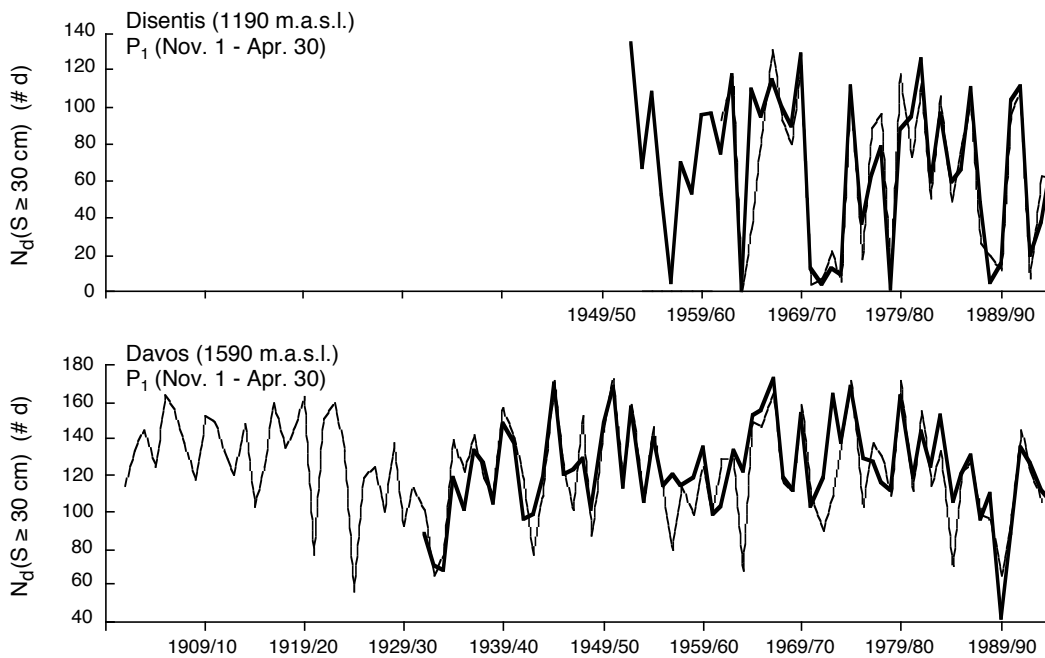


491

492

493

**Figure 3:** Comparison of measured (thick lines) and simulated (thin lines) long-term mean daily snow depths at Disentis (top) and Davos (bottom).



494

495

496

497

498

**Figure 4:** Comparison of measured (thick lines) and simulated (thin lines) numbers of days at which snow depth exceeds 30 cm in subperiod  $P_1$  (Nov. 1 - Apr. 30) at Disentis (top) and Davos (bottom). The parameters of the snow model were fitted for the winters 1981/82-1994/95, those of the temporal downscaling procedure for the years 1981-1985.

499 **Table 4:** Validation results for the numbers of days at which snow depth exceeds a given threshold

Site	n	Statistic	P <sub>1</sub> (Nov. 1 - Apr. 30)						P <sub>2</sub> (Dec. 1 - Apr. 15)						P <sub>3</sub> (Dec. 20 - Dec. 31)					
			h	0	10	20	30	40	50	0	10	20	30	40	50	0	10	20	30	40
Engelberg	11	r	<u>.87</u>	<u>.53</u>	<u>.56</u>	<u>.81</u>	<u>.87</u>	<u>.87</u>	<u>.81</u>	.47	<u>.53</u>	<u>.80</u>	<u>.88</u>	<u>.88</u>	<u>.79</u>	<u>.79</u>	<u>.53</u>	<u>.88</u>	<u>.61</u>	<u>.29</u>
		Δ	3.1	-1.0	2.4	1.6	2.7	0.7	0.5	-2.1	1.0	0.3	1.4	-0.3	0.8	0.0	-0.1	0.1	0.9	0.5
		Δ%	2	-1	4	4	10	4	0	-2	2	1	5	-2	8	1	-1	4	88	131
Disentis	20	r	<u>.91</u>	<u>.92</u>	<u>.89</u>	<u>.88</u>	<u>.87</u>	<u>.86</u>	<u>.91</u>	<u>.91</u>	<u>.89</u>	<u>.89</u>	<u>.88</u>	<u>.86</u>	<u>.54</u>	<u>.76</u>	<u>.72</u>	<u>.66</u>	<u>.86</u>	<u>.82</u>
		Δ	0.7	-1.5	-3.2	-1.8	0.4	-0.5	0.8	-0.9	-3.2	-2.7	-0.5	-1.1	1.4	0.9	-0.3	-0.4	0.1	-0.3
		Δ%	1	-1	-4	-3	1	-1	1	-1	-4	-4	-1	-3	15	11	-4	-8	3	-13
Montana	30	r	<u>.77</u>	<u>.91</u>	<u>.88</u>	<u>.87</u>	<u>.88</u>	<u>.88</u>	<u>.79</u>	<u>.91</u>	<u>.86</u>	<u>.85</u>	<u>.89</u>	<u>.89</u>	<u>.50</u>	<u>.72</u>	<u>.65</u>	<u>.75</u>	<u>.84</u>	<u>.78</u>
		Δ	-4.4	-8.3	-10.5	-11.5	-10.7	-10.1	-6.0	-8.5	-10.4	-11.2	-11.0	-10.7	0.0	-0.6	-0.7	0.1	0.3	0.0
		Δ%	-3	-7	-9	-11	-12	-12	-5	-8	-10	-12	-13	-14	0	-7	-9	1	7	-1
Davos	51	r	<u>.72</u>	<u>.76</u>	<u>.75</u>	<u>.80</u>	<u>.86</u>	<u>.90</u>	<u>.32</u>	<u>.54</u>	<u>.61</u>	<u>.68</u>	<u>.84</u>	<u>.89</u>	NA	.11	<u>.61</u>	<u>.72</u>	<u>.88</u>	<u>.90</u>
		Δ	-0.3	-1.9	-2.4	-2.5	-1.7	3.9	-1.4	-1.5	-1.6	-2.3	-2.3	2.8	0.0	0.0	0.2	0.5	0.2	0.9
		Δ%	0	-1	-2	-2	-2	4	-1	-1	-1	-2	-2	3	0	0	2	6	3	23
Weissfluhjoch	10	r	(.01)	(.01)	(-.01)	(.00)	<u>.72</u>	<u>.68</u>	( <u>.85</u> )	(.45)	(.35)	(.33)	(.32)	(.01)	NA	NA	NA	NA	NA	NA
		Δ	-1.4	-3.3	-5.5	-7.1	-7.2	-12.6	-0.1	-0.6	-1.1	-1.8	-2.9	-7.0	0.0	0.0	0.0	-0.1	-0.5	-1.8
		Δ%	-1	-2	-3	-4	-4	-7	0	0	-1	-1	-2	-5	0	0	0	-1	-4	-15

500 n: number of winters considered for validation; r: Pearson product-moment correlation coefficient between the simulated  
501 (sim) and the observed (obs) time series of numbers of days within a given subperiod (P<sub>i</sub>) of the year at which snow depth  
502 exceeds a given threshold h; Δ: mean deviation = (1/n)∑(sim<sub>i</sub>-obs<sub>i</sub>); Δ%: mean relative deviation = (1/n)∑[100(sim<sub>i</sub>-  
503 obs<sub>i</sub>)/obs<sub>i</sub>]; h: snow depth threshold (in cm); P<sub>1</sub>-P<sub>3</sub>: subperiods of the year considered; NA: statistic not available; x, x,  
504 and x denote r values which are significantly different from zero at the 90%, 95% and 99% confidence levels, respectively  
505 (two-tailed test, H<sub>0</sub>: r=0). Brackets denote cases where the coefficient of variation of the measured time series is below 5%.

506 **Table 5:** Validation results for the relative frequencies of years with selected snow cover characteristics

Site	Statistic	RF[ N <sub>d</sub> (S ≥ h) < 40 d ]						RF[ N <sub>d</sub> (S ≥ h) ≥ 100 d ]						RF[ N <sub>d</sub> (S ≥ h) ≥ 10 d ]						
		P <sub>2</sub> (Dec. 1 - Apr. 15)						P <sub>2</sub> (Dec. 1 - Apr. 15)						P <sub>3</sub> (Dec. 20 - Dec. 31)						
		h	0	10	20	30	40	50	0	10	20	30	40	50	0	10	20	30	40	50
Engelberg	RF <sub>Obs</sub>	0	0	36	36	82	91	82	27	9	9	0	0	73	55	27	18	0	0	
	RF <sub>Sim</sub>	0	9	36	55	64	91	82	18	9	0	0	0	73	27	18	9	0	0	
	Δ	0	9	0	<b>18</b>	<b>-18</b>	0	0	-9	0	-9	0	0	0	<b>-27</b>	-9	-9	0	0	
Disentis	RF <sub>Obs</sub>	0	5	30	35	40	40	75	55	45	30	10	0	75	65	50	35	20	20	
	RF <sub>Sim</sub>	0	10	35	40	40	50	75	60	40	25	10	5	85	65	40	20	15	10	
	Δ	0	5	5	5	0	10	0	5	-5	-5	0	5	10	0	-10	<b>-15</b>	-5	-10	
Montana	RF <sub>Obs</sub>	0	3	7	10	10	24	90	83	72	59	45	31	83	72	59	45	34	24	
	RF <sub>Sim</sub>	0	10	10	17	23	30	83	63	57	43	43	37	80	60	57	40	30	23	
	Δ	0	7	3	6	<b>13</b>	6	-6	<b>-19</b>	<b>-16</b>	<b>-15</b>	-1	6	-3	<b>-12</b>	-2	-5	-4	-1	
Davos	RF <sub>Obs</sub>	0	0	0	0	4	10	100	100	96	80	62	36	100	96	80	60	48	26	
	RF <sub>Sim</sub>	0	0	0	0	2	8	100	100	92	76	55	43	100	92	73	55	39	31	
	Δ	0	0	0	0	-2	-2	0	0	-4	-4	-7	7	0	-4	-7	-5	-9	5	
Weissfluhjoch	RF <sub>Obs</sub>	0	0	0	0	0	0	100	100	100	100	100	100	100	100	100	100	100	100	
	RF <sub>Sim</sub>	0	0	0	0	0	0	100	100	100	100	100	100	100	100	100	100	90	80	
	Δ	0	0	0	0	0	0	0	0	0	0	0	0	0	0	0	0	-10	<b>-20</b>	

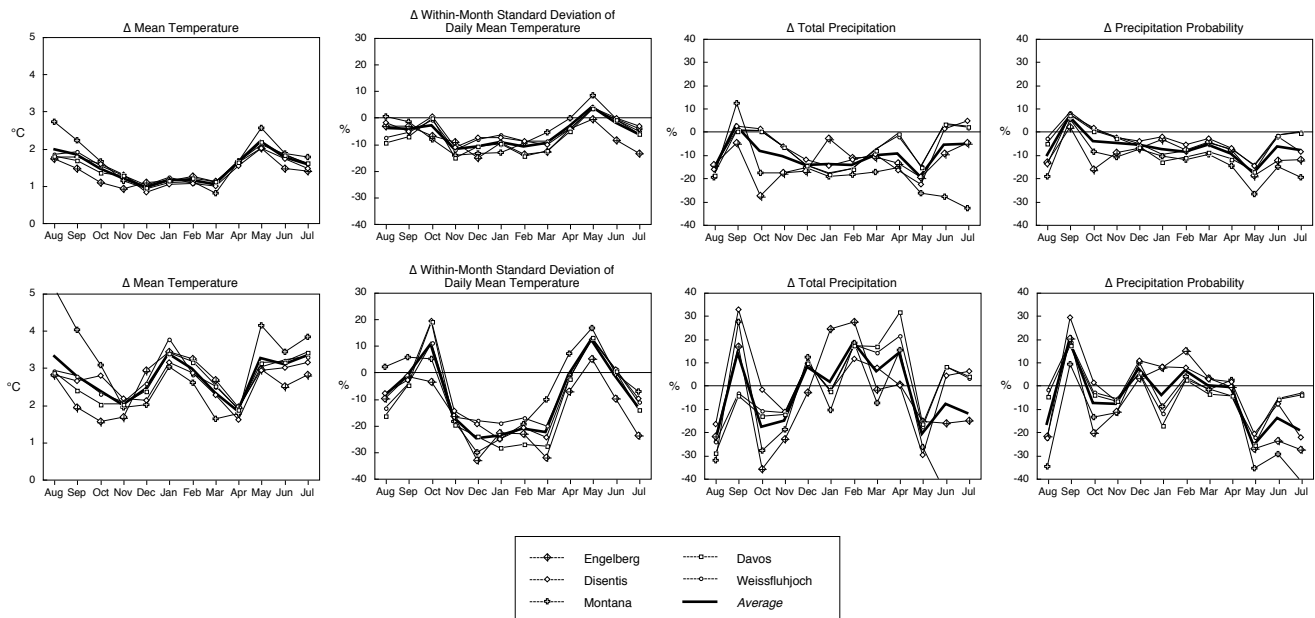
507 RF<sub>Obs</sub>, RF<sub>Sim</sub>: measured and simulated relative frequencies in the validation period, respectively; Δ: RF<sub>Sim</sub> minus  
508 RF<sub>Obs</sub>; h: snow depth threshold (in cm); N<sub>d</sub>(S ≥ h): number of days within a given subperiod (P<sub>i</sub>) of the year at which  
509 snow depth (S) exceeds h; P<sub>2</sub>, P<sub>3</sub>: subperiods of the year considered. All data are given in % and were computed using  
510 varying numbers of winters depending on the location (see Section 2.8). Deviations larger than 10% are shown in bold.

511 A quantitative assessment of the model's performance is given in Table 4, which compiles  
 512 the validation results for  $N_d(S \geq h)$ . The correlation coefficients ( $r$ ) between the observed  
 513 and simulated  $N_d$  time series were generally highly significant. The mean ( $\Delta$ ) and mean  
 514 relative ( $\Delta\%$ ) errors were typically less than 3 d and 10%, respectively. Some larger  
 515 negative biases were however obtained for Montana and Weissfluhjoch for the subperiods  
 516  $P_1$  and  $P_2$ .

517 Table 5 shows the validation results for selected RF statistics. In 80 of the  $3 \times 6 \times 5 = 90$   
 518 conducted comparisons the differences between the observed and simulated statistics were  
 519 below 10%. Errors larger than 10% occurred in 9 out of 52 cases where the observed RF  
 520 was between 5% and 95%. The largest deviations were obtained for Engelberg and  
 521 Montana, and for Weissfluhjoch in subperiod  $P_3$ . The simulations generally tended to  
 522 overestimate the RFs of the "bad years" for skiing ( $N_d < 40$ ) and to underestimate the RFs  
 523 of the "good years".

### 524 3.2 Climate Change Scenarios from Spatial Downscaling

525 Fig. 5 shows the results obtained from the spatial downscaling procedure for selected  
 526 climate parameters and the two GCM simulations. The ECHAM scenario (upper panels)  
 527 specified a slightly warmer and drier wintertime climate as compared to the 1931-1980  
 528 conditions, whereas the CCC scenario (bottom panels) suggested a shift towards  
 529 substantially warmer and wetter winters. Both scenarios specified a decrease for the  
 530 within-month standard deviation of wintertime daily mean T. This decrease was more  
 531 pronounced under the CCC scenario. Wintertime Pprob was found to systematically  
 532 decrease in the ECHAM scenario, but it showed small or no changes in the CCC scenario.



533

534 **Figure 5:** Changes ( $\Delta$ ) in selected climatic parameters according to the ECHAM (top) and  
 535 CCC (bottom) climatic scenarios. All changes are given relative to the 1931-1980 baseline.  
 536 See also Table 6.

537  
538**Table 6:** Average climatic changes for the winter half-year (November-April) according to the ECHAM and CCC climatic scenarios

Scenario / Location	$\Delta T_{\text{mean}}$ (°C)	$\Delta T_{\text{min}}$ (°C)	$\Delta T_{\text{max}}$ (°C)	$\Delta \text{SDT}_{\text{m}}$ (%)	$\Delta \text{SDT}_{\text{n}}$ (%)	$\Delta \text{SDT}_{\text{x}}$ (%)	$\Delta \text{Precip}$ (%)	$\Delta \text{Pprob}$ (%)
ECHAM								
Engelberg	1.19	1.36	1.03	-10.7	-10.7	-10.7	-12.5	-6.9
Disentis	1.13	0.96	1.12	-8.2	-8.4	-9.1	-12.2	-4.4
Montana	1.12	1.12	1.21	-9.3	-9.9	-6.9	-17.6	-11.2
Davos	1.22	1.22	1.29	-11.3	-10.0	-11.0	-10.8	-9.1
Weissfluhjoch	1.23	1.24	1.07	-8.2	-6.5	-10.5	-10.8	-6.6
<i>Average</i>	<i>1.18</i>	<i>1.18</i>	<i>1.15</i>	<i>-9.5</i>	<i>-9.1</i>	<i>-9.6</i>	<i>-12.8</i>	<i>-7.6</i>
CCC								
Engelberg	2.63	2.80	2.46	-22.4	-21.1	-21.1	4.2	2.9
Disentis	2.35	2.13	2.19	-17.7	-17.1	-18.7	2.7	4.0
Montana	2.14	2.25	2.15	-16.0	-17.2	-10.9	1.5	-0.9
Davos	2.55	2.59	2.52	-21.6	-18.1	-20.9	10.1	-4.0
Weissfluhjoch	2.60	2.57	2.18	-15.4	-10.1	-15.3	8.2	-2.5
<i>Average</i>	<i>2.45</i>	<i>2.47</i>	<i>2.30</i>	<i>-18.6</i>	<i>-16.7</i>	<i>-17.4</i>	<i>5.3</i>	<i>-0.1</i>

539  
540  
541  
542  
543

Shown are changes relative to the 1931-1980 baseline.  $\Delta T_{\text{mean}}$ ,  $\Delta T_{\text{min}}$ ,  $\Delta T_{\text{max}}$ : changes in the monthly mean, mean daily minimum, and mean daily maximum temperature;  $\Delta \text{SDT}_{\text{m}}$ ,  $\Delta \text{SDT}_{\text{n}}$ ,  $\Delta \text{SDT}_{\text{x}}$ : changes in the within-month standard deviations of the daily mean, daily minimum and daily maximum temperatures;  $\Delta \text{Precip}$ : change in monthly total precipitation;  $\Delta \text{Pprob}$ : change in monthly precipitation probability. See also Figure 5.

544  
545  
546  
547  
548  
549  
550

The winter half-year average changes that were obtained from spatial downscaling for the 8 monthly input variables of relevance to the snow cover simulations are summarized in Table 6. In the ECHAM scenario the temperature minima showed at three locations smaller changes as compared to the maxima, whereas in the CCC scenario the minima showed similar or larger changes than the maxima. The within-month standard deviations of the three T variables generally showed changes of similar magnitude for a given location and scenario.

551

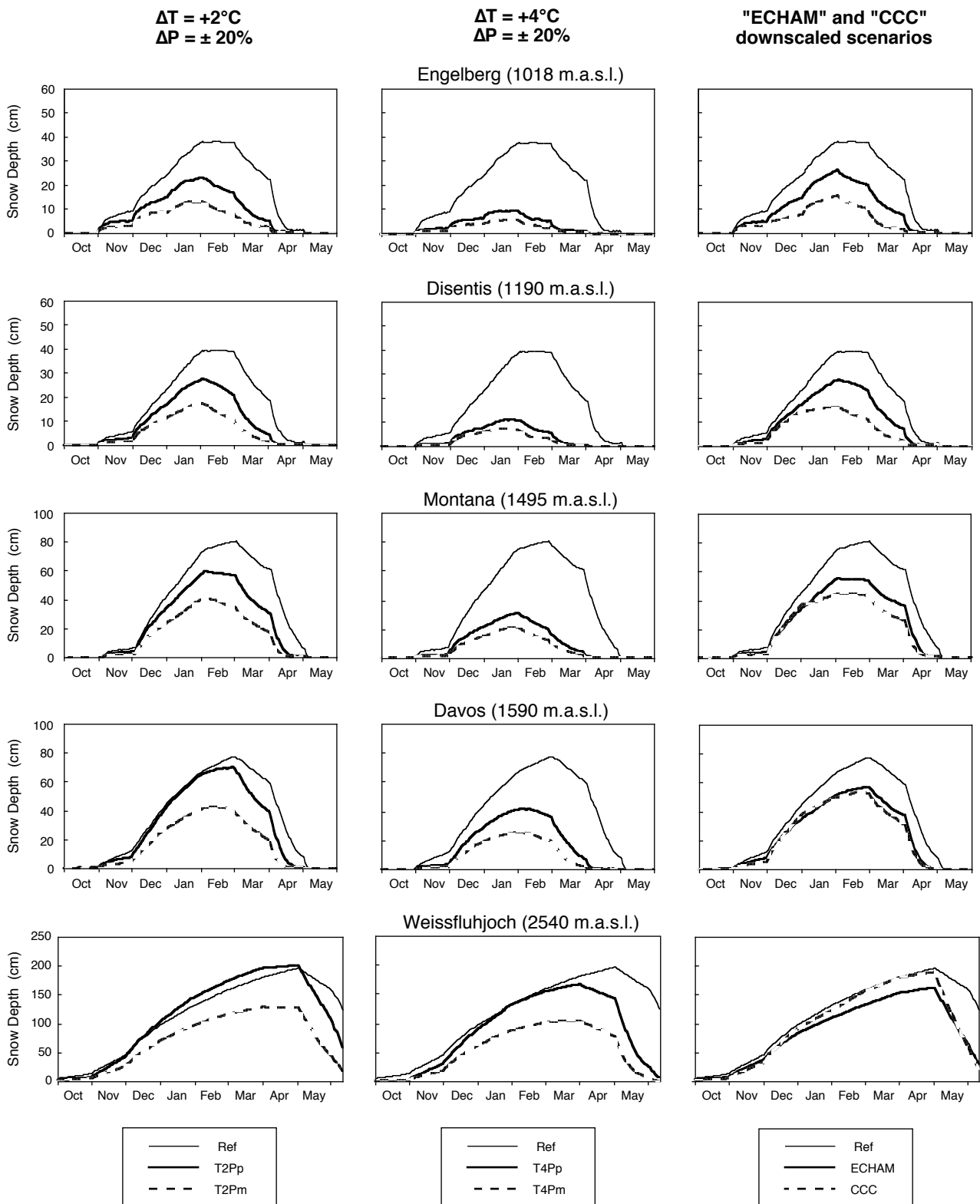
### 3.3 Climatic Sensitivity of Snow Depth Statistics

552  
553

The simulated responses of the long-term mean seasonal cycles of S to the various climate change scenarios are shown in Fig. 6. Several observations can be made:

554  
555  
556  
557  
558  
559  
560  
561  
562  
563  
564  
565  
566  
567

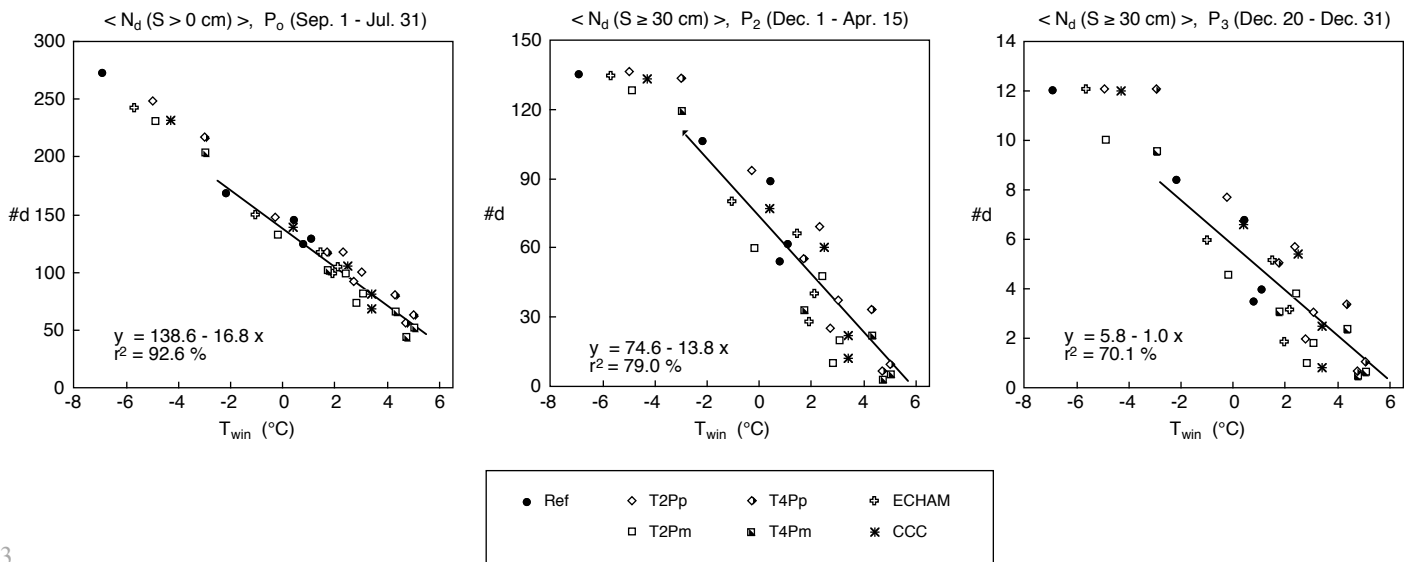
First, the simulations specified a general decrease in S. An exception occurred for the scenarios T2Pp, T4Pp and CCC at Weissfluhjoch, where only small changes or even slight increases were obtained for the period from October through March or April. Second, the T2 scenarios always yielded smaller changes than their T4 counterparts that assumed the same changes in P. Third, for a given change in T the Pm scenarios yielded generally larger decreases than the Pp scenarios. The effect of the Pm scenarios was more pronounced under the T2 scenarios as compared to the T4 scenarios, and it increased with elevation. Fourth, the relative response to the two GCM-downscaled scenarios also showed a clear elevation dependency: The CCC scenario yielded a stronger signal than the ECHAM scenario at the three lowest sites, but the differences decreased with elevation and at the high-elevation site Weissfluhjoch they were even reversed. Finally, from Fig. 6 it can be seen that the largest decreases in long-term mean snow cover were typically obtained in spring, such that in most cases the date of the maximum snow depth was shifted towards earlier in the winter season.



568

569  
570  
571  
572

**Figure 6:** Effect of different climate change scenarios on simulated long-term mean daily snow depths at the five case study sites. Ref: simulated snow depths for the reference (present-day) climate, winters 1981/82-1994/95 (cf. Figure 3); T2Pp, T2Pm, T4Pp, T4Pm, ECHAM, CCC: simulated snow depths under the respective scenarios of climatic change.



573

574 **Figure 7:** Simulated long-term mean numbers of days ( $\langle N_d(\dots) \rangle$ ) at which snow depth ( $S$ )  
 575 exceeds a given threshold (0 or 30 cm) within selected subperiods ( $P_0$ ,  $P_2$  or  $P_3$ ) of the year  
 576 as a function of winter half-year (November-April) long-term mean temperature ( $T_{win}$ ). Ref:  
 577 simulated values for the reference (present-day) climate, winters 1981/82-1994/95; T2Pp,  
 578 T2Pm, T4Pp, T4Pm, ECHAM, CCC: simulated values under the respective scenarios of  
 579 climatic change. See also Table 7.

580 **Table 7:** Simulated temperature sensitivities for the long-term mean numbers of days at which snow depth exceeds a given  
 581 threshold within selected subperiods of the year

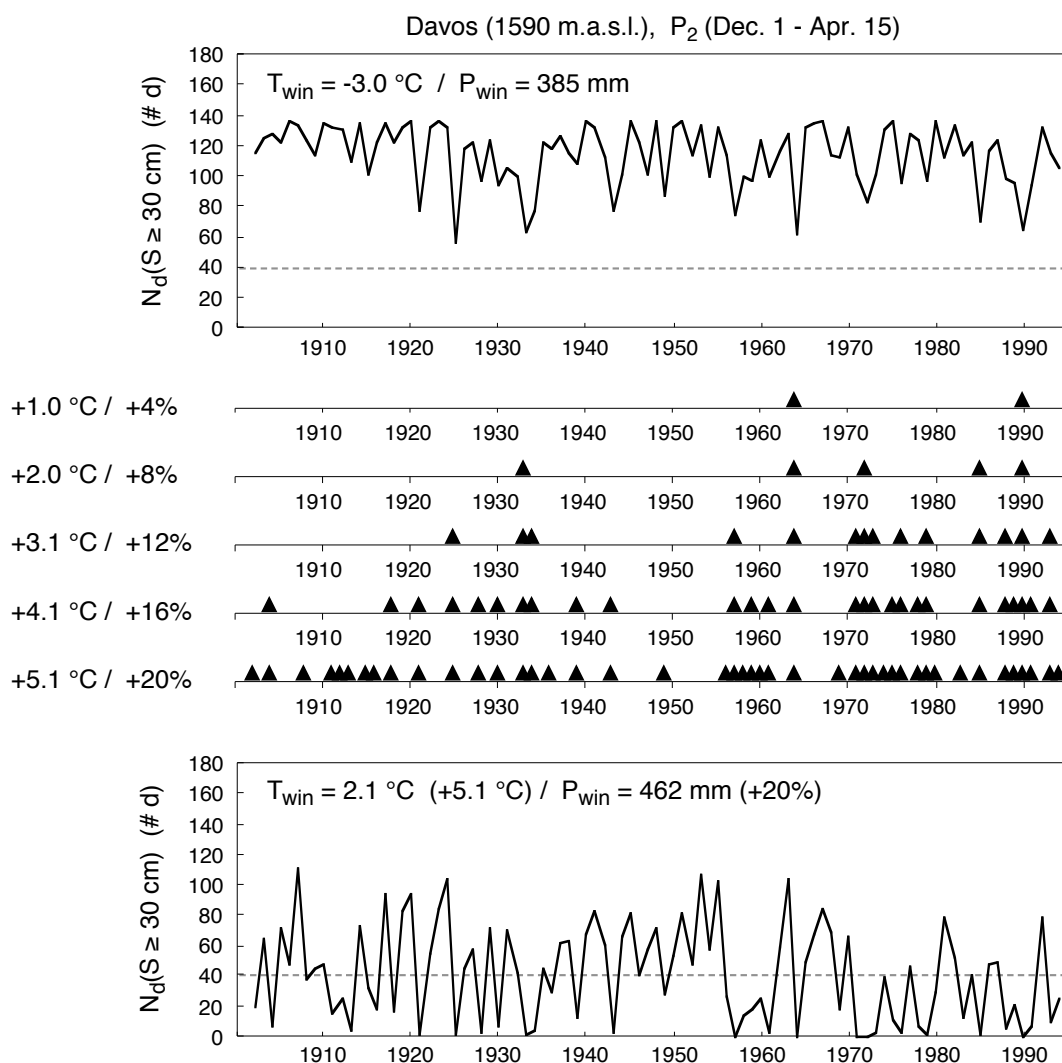
h (cm)	$P_0$ (Oct. 1 - May 31)				$P_2$ (Dec. 1 - Apr. 15)				$P_3$ (Dec. 20 - Dec. 31)			
	$\langle \bar{N}_d \rangle$ (#d)	AS (#d/ $^{\circ}C$ )	RS (%/ $^{\circ}C$ )	$r^2$ (%)	$\langle \bar{N}_d \rangle$ (#d)	AS (#d/ $^{\circ}C$ )	RS (%/ $^{\circ}C$ )	$r^2$ (%)	$\langle \bar{N}_d \rangle$ (#d)	AS (#d/ $^{\circ}C$ )	RS (%/ $^{\circ}C$ )	$r^2$ (%)
0	101.0	-16.8	-16.6	92.6	88.4	-12.9	-14.6	88.2	9.0	-1.0	-11.6	77.0
10	72.2	-16.6	-22.9	87.0	67.6	-14.9	-22.0	85.3	6.6	-1.3	-20.1	78.8
20	56.3	-15.7	-27.8	83.1	54.2	-14.8	-27.3	82.4	4.8	-1.2	-25.0	74.5
30	44.6	-14.3	-32.0	79.3	43.6	-13.8	-31.7	79.0	3.6	-1.0	-28.4	70.1
40	35.4	-12.6	-35.6	75.2	34.9	-12.3	-35.3	75.1	2.6	-0.8	-30.4	65.8
50	28.1	-10.9	-38.8	70.6	27.9	-10.7	-38.6	70.6	1.9	-0.6	-31.5	59.1

582  $P_0, P_2, P_3$ : subperiods of the year considered; h: snow depth threshold;  $\langle \bar{N}_d \rangle$ : average for all sites and scenarios used to  
 583 compute sensitivities of the long-term mean number of days ( $\langle N_d \rangle$ ) within a given subperiod ( $P_i$ ) of the year at which snow  
 584 depth exceeds h; AS: absolute sensitivity,  $\partial \langle N_d \rangle / \partial T_{win}$ , where  $T_{win}$  = winter half-year (November-April) long-term mean  
 585 temperature; RS: relative sensitivity,  $(\partial \langle N_d \rangle / \partial T_{win}) / \langle \bar{N}_d \rangle$ ;  $r^2$ : percentage of variance explained by the linear regression used  
 586 to estimate  $\partial \langle N_d \rangle / \partial T_{win}$ . Results were based on simulated snow depths at the sites Engelberg, Disentis, Montana and  
 587 Davos under present-day and changed climatic conditions according to the scenarios T2Pp, T2Pm, T4Pp, T4Pm, ECHAM  
 588 and CCC. The average  $T_{win}$  for the four sites and all scenarios was  $2.2 \text{ }^{\circ}C$ . All sensitivities apply to the temperature range  
 589  $-2.2 \text{ }^{\circ}C$  to  $+5.1 \text{ }^{\circ}C$ . See also Figure 7.

590 Fig. 7 shows the simulated long-term means ( $\langle N_d \rangle$ ) of selected  $N_d(S \geq h)$  statistics as a  
 591 function of  $T_{win}$ . The  $\langle N_d \rangle$  for the days with snow lying on the ground (top left panel)  
 592 was found to decrease by  $\sim 17 \text{ d per } ^{\circ}C$  change in  $T_{win}$ . In most cases the  $\langle N_d \rangle$  were

593 found to remain close to their respective maximum values for  $T_{win}$  below ca.  $-2\text{ }^{\circ}\text{C}$ , but  
 594 above this threshold they showed a more or less linear decrease with increasing  $T_{win}$ .

595 The sensitivities  $\partial\langle N_d \rangle / \partial T_{win}$  for various subperiods of the year and snow depth  
 596 thresholds are summarized in Table 7. The sensitivities were estimated using all data  
 597 points that fall between the two extreme states  $\langle N_d \rangle = \text{maximum number of days}$  (Table  
 598 3) and  $\langle N_d \rangle = 0$ . It can be seen that the AS tended to decrease with increasing snow  
 599 depth  $h$ , whereas for the RS was found the opposite result. The robustness of the  
 600 sensitivity estimates (as measured by the  $r^2$  of the regressions) was also found to decrease  
 601 with increasing  $h$  and with decreasing length of the subperiod of the year considered.

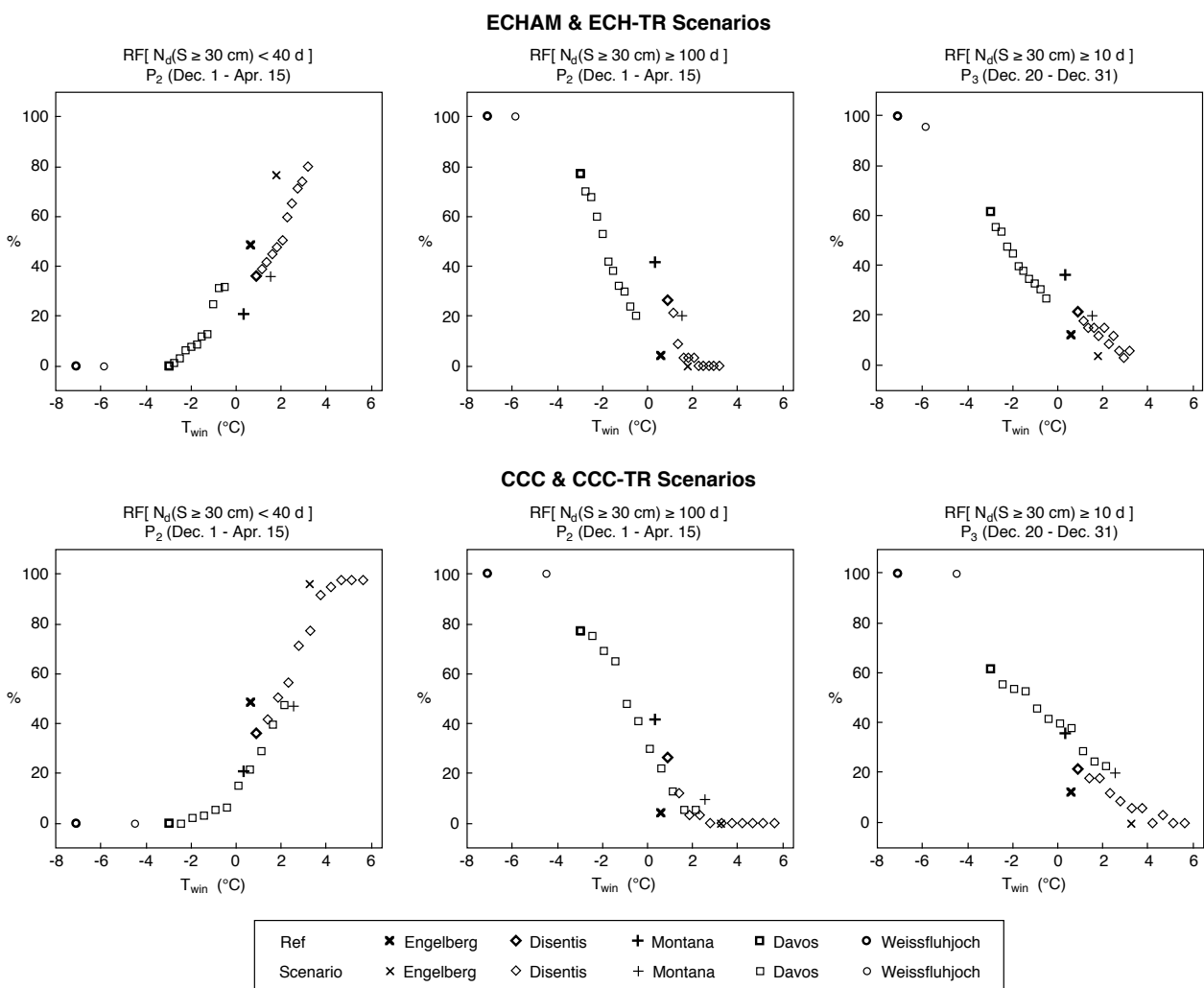


602

603 **Figure 8:** Simulated numbers of days at which snow depth exceeds 30 cm in the subperiod  
 604 P<sub>2</sub> (Nov. 1 - Apr. 30) at Davos under present conditions (top panel) and under the CCC-  
 605 TR(s=2.0) scenario (bottom panel). The panels inbetween show the years with simulated  
 606 number of days < 40 d (event signified by ▲) for the scenarios CCC-TR(s=0.4) to CCC-  
 607 TR(s=2.0), with s varying in steps of 0.4 ("s" denotes the factor used to scale the original  
 608 CCC scenario, see Section 2.8).  $T_{win}$ ,  $P_{win}$ : winter half-year (November-April) long-term  
 609 mean temperature and precipitation, respectively; xx °C / yy %: assumed changes in  $T_{win}$  /  
 610  $P_{win}$  under the respective scenario.

611 Fig. 8 shows the simulated  $N_d(S \geq 30 \text{ cm})$  time series for Davos in subperiod  $P_2$  under  
 612 present (top panel) and CCC-TR(2.0) (bottom panel) scenario conditions. The panels in  
 613 between indicate the occurrence of "bad" years for skiing for a subset of the CCC-TR  
 614 scenarios. It can be seen that the "bad" years' frequency increased over-proportionally  
 615 with increasing  $T_{win}$ .

616 From the comparison of the top and bottom panels in Fig. 8 it can further be discerned  
 617 that the assumed changes in climate lead to distinct shifts in the shape of the snow  
 618 variables' statistical distribution. For instance, the standard deviation of the simulated  $N_d$   
 619 was found to increase from 20.4 d under present conditions (top panel) to 31.7 d under the  
 620 CCC-TR(2.0) scenario (bottom panel, +56%), and the skewness of the time series changed  
 621 from -0.97 (top panel) to +0.33 (bottom panel).



622

623 **Figure 9:** Simulated relative frequencies (RF) of years with selected snow cover  
 624 characteristics as a function of winter half-year (November-April) long-term temperature  
 625 ( $T_{win}$ ).  $N_d(S \geq h)$ : number of days at which snow depth exceeds  $h$ ;  $P_2$ ,  $P_3$ : subperiods of  
 626 the year considered; Ref: simulated relative frequencies for the reference (present-day) climate;  
 627 ECHAM, ECH-TR, CCC, CCC-TR: simulated relative frequencies under the respective  
 628 scenarios of climatic change. The simulations considered a varying number ( $\geq 24$ ) of winters,  
 629 depending on the location (see Section 2.7). See also Table 8.

630 **Table 8:** Simulated temperature sensitivities for the relative frequencies of years with selected snow cover  
 631 characteristics

h (cm)	RF[ $N_d(S \geq h) < 40$ d ] P <sub>2</sub> (Dec. 1 - Apr. 15)				RF[ $N_d(S \geq h) \geq 100$ d ] P <sub>2</sub> (Dec. 1 - Apr. 15)				RF[ $N_d(S \geq h) \geq 10$ d ] P <sub>3</sub> (Dec. 20 - Dec. 31)			
	$\overline{RF}$ (%)	Range $T_{win}$ (°C)	AS (%/°C)	$r^2$ (%)	$\overline{RF}$ (%)	Range $T_{win}$ (°C)	AS (%/°C)	$r^2$ (%)	$\overline{RF}$ (%)	Range $T_{win}$ (°C)	AS (%/°C)	$r^2$ (%)
0	20.2	+1.6..+5.7	14.3	83.3	54.0	-1.0..+3.8	-18.8	83.5	63.1	-0.8..+5.7	-10.1	54.8
10	31.9	-0.8..+5.2	14.7	82.7	47.0	-2.2..+2.9	-15.7	86.5	54.0	-3.0..+5.7	-11.1	81.8
20	39.9	-1.5..+4.8	13.6	79.3	46.8	-3.0..+2.6	-14.3	84.5	37.9	-3.0..+5.2	-9.9	82.5
30	42.2	-2.2..+4.3	13.1	82.4	36.6	-3.0..+2.6	-12.5	81.4	28.2	-3.0..+3.8	-8.0	86.3
40	45.8	-2.7..+3.8	13.3	85.5	29.1	-3.0..+2.6	-9.5	76.6	25.4	-6.6..+2.6	-6.4	88.6
50	52.2	-3.0..+3.3	12.7	85.9	26.3	-6.6..+1.6	-8.7	84.7	24.2	-7.8..+2.6	-7.5	83.4

632 RF: relative frequency;  $N_d(S \geq h)$ : number of days within a given subperiod ( $P_i$ ) of the year at which snow depth  
 633 (S) exceeds h;  $P_2$ ,  $P_3$ : subperiods of the year considered;  $\overline{RF}$ : average RF for all sites and scenarios used to  
 634 compute a sensitivity;  $T_{win}$ : winter half-year (November-April) long-term mean temperature; AS: absolute  
 635 sensitivity  $\partial RF / \partial T_{win}$ ;  $r^2$ : percentage of variance explained by the linear regression used to estimate  $\partial RF / \partial T_{win}$ .  
 636 Results were based on simulated snow depths under present-day and changed climatic conditions according to the  
 637 scenarios ECHAM and CCC (all five case study sites), plus scenarios ECH-TR and CCC-TR (sites Disentis and  
 638 Davos only). The simulations considered a varying number ( $\geq 24$ ) of winters, depending on the location (see  
 639 Section 2.7). The sensitivities were determined using simulation results from all sites and scenarios for which  
 640  $T_{win}$  fell within the specified range. See also Figure 9.

641 Generally, changes in the interannual variability of the various  $N_d$  time series were found  
 642 to depend on the threshold h, the subperiod of the year, and  $T_{win}$  (results not shown). On  
 643 average over all locations and scenarios, the variability was found to increase with  
 644 increasing  $T_{win}$  up to a certain critical value,  $T_{crit}$ , and then to decrease again above this  
 645 value.  $T_{crit}$  tended to decrease with increasing h and with increasing length of the  
 646 subperiod used to compute the snow depth statistics. For instance, for h = 0 cm and  $P_0$   
 647 was  $T_{crit} = 2.9$  °C, and for  $P_3$  was  $T_{crit} = 4.2$  °C; for h = 30 cm  $T_{crit}$  ranged between -0.2  
 648 °C and +0.9 °C; and for h = 50 cm it was between -1.2 °C and -0.6 °C.

649 Fig. 9 shows selected RF statistics as a function of  $T_{win}$ . The RFs of the simulated "bad"  
 650 years for skiing (left panels) were generally found to increase, and the RFs of the "good  
 651 years" (middle and right panels) to decrease with rising  $T_{win}$ . The average rates of change  
 652 per degree change in  $T_{win}$  depended somewhat on the choice of the scenario and statistic.  
 653 For instance the RFs of the "good years" were found to decrease more strongly under the  
 654 ECHAM and ECH-TR scenarios (top panels in Fig. 8) as compared to the CCC and CCC-  
 655 TR scenarios (bottom panels).

656 Table 8 gives a summary of the simulated average sensitivities  $\partial RF / \partial T_{win}$ . They were  
 657 estimated using all RF values in the range 5% to 95%. The sensitivities of the "bad" years  
 658 for skiing (Table 8, left) were found to slightly decrease with increasing snow depth  
 659 threshold h. An even stronger decrease of sensitivity with h was obtained for the "good"  
 660 years (Table 8, middle and right). The  $r^2$  of the regressions were generally above 75%; the  
 661 only exception occurred for h = 0 cm and subperiod  $P_3$ . In this case only a limited sample  
 662 of RF values above 5% was available to estimate the  $\partial RF / \partial T_{win}$  (not shown).

663

### 3.4 Comparison with Earlier Swiss Studies

664 BULTOT et al. (1992) used the daily time step, lumped-parameter conceptual model IRMB  
 665 to study changes in the hydrology of the Murg basin in northern Switzerland (212 km<sup>2</sup>,  
 666 elevation range 390-1035 m, average 580 m). They assumed changes in  $T_{win}$  by +3.2 °C  
 667 and in winter total precipitation ( $P_{win}$ ) by +11%, and obtained for long-term mean  $N_d(S >$   
 668 0 cm) in subperiod  $P_0$  AS = -18.2 d/°C and RS = -23 %/°C (their Table 2). This compares  
 669 with AS = -16.6 d/°C and RS = -16.6 %/°C reported in Table 7.

670 BULTOT et al. (1994) applied the IRMB model also to the Broye catchment in western  
 671 Switzerland (392 km<sup>2</sup>, 441-1514 m, average 710 m). They considered a seasonally  
 672 uniform warming by 1 °C and 2 °C, respectively, with no changes in precipitation, plus  
 673 the same climate change scenario as BULTOT et al. (1992). Their simulations yielded for  
 674 long-term mean  $N_d(S > 0$  cm) in subperiod  $P_0$  and on average over the two elevation zones  
 675 900-1200 m and 1200-1500 m AS = -22.8 d/°C, RS = -18 %/°C (their Table III). For our  
 676 three lowest locations (1018-1495 m) we obtained AS = -18.4 d/°C and RS = -21 %/°C  
 677 (not shown). For long-term mean  $N_d(S \geq 30$  cm) in the subperiod December to April and  
 678 the elevation zone 1200-1500 m their work yielded AS = -19.3 d/°C, RS = -21%/°C (their  
 679 Table IV). Our result for the same elevation range (i.e., locations Disentis and Montana)  
 680 and the subperiod  $P_2$  was AS = -15.6 d/°C, RS = -38 %/°C.

681 SCHULLA (1997) investigated possible changes in the hydrology of the Thur catchment in  
 682 northern Switzerland (1700 km<sup>2</sup>, 356-2504 m, average 769 m) using the WaSiM-ETH  
 683 distributed parameter model. He used three climate change scenarios that assumed changes  
 684 in  $T_{win}$  by +1.2 °C, +2.3 °C and +2.9 °C, and in  $P_{win}$  by +11%, +9% and +16%,  
 685 respectively. His simulations (his Fig. 4.13) give for long-term mean  $N_d(S \geq 10$  cm) in  
 686 subperiod  $P_0$  and the elevation range 1100-1700 m AS = -25.8 d/°C and RS = -29 %/°C.  
 687 Our corresponding estimates (Table 6) were AS = -16.6 d/°C, RS = -23 %/°C. For long-  
 688 term mean  $N_d(S \geq 30$  cm) he obtained -21.8 d/°C (-42 %/°C) whereas our simulations  
 689 (Table 7) yielded -14.3 d/°C (-32 %/°C).

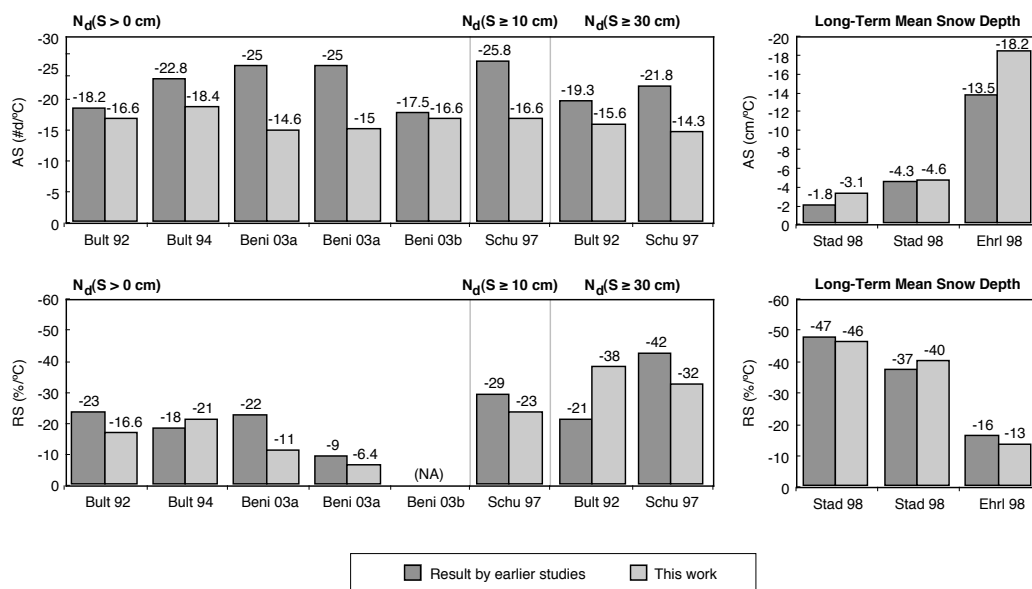
690 STADLER et al. (1998) employed the SOIL one-dimensional coupled mass and heat transfer  
 691 model for point hydrological simulations at the sites Engelberg and Davos. They used two  
 692 incremental scenarios that assumed a seasonally uniform temperature increase by 1.5 °C  
 693 and 3 °C, respectively, and no changes in precipitation, plus two scenarios that specified  
 694 site-specific changes for  $T_{win}$  and  $P_{win}$  (Engelberg: +1.3 °C, -11% and +2.2 °C, -11%;  
 695 Davos: +1.0 °C, -3%, +1.8 °C, +6%). For long-term mean annual mean snow depth at  
 696 Engelberg they obtained AS = -1.8 cm/°C, RS = -47 %/°C and for Davos AS = -4.3 cm/°C,  
 697 RS = -37 %/°C (their Tables 4.1 and 4.2). The corresponding average values from our  
 698 simulations were for Engelberg -3.1 cm/°C (-46 %/°C) and for Davos -4.6 cm/°C (-40  
 699 %/°C) (not shown, cf. Fig. 6).

700 EHRLER (1998; see also SEIDEL et al. 1998) used the SRM semi-distributed (elevation  
 701 zones) conceptual model to simulate possible changes in snow accumulation and runoff for  
 702 the Upper Rhine basin in central/eastern Switzerland (3250 km<sup>2</sup>, 560-3614 m, average  
 703 2000 m; our sites Disentis, Davos and Weissfluhjoch are located within this basin). He  
 704 employed 15 climatic scenarios which specified seasonally uniform changes in  $T_{win}$   
 705 between 0 °C and 3.8 °C and in  $P_{win}$  between 0% and +20%. For the areal mean, long-  
 706 term mean water equivalent of the snow cover in the elevation range 1100-2600 m his  
 707 study gave AS = -6.0 cm/°C, RS = -16%/°C (his Table 29). Assuming an average snow  
 708 density of 0.4 to 0.5 kg/m<sup>3</sup> this AS value translates to a sensitivity for the annual mean

709 snow depth of -12 to -15 cm/°C. The corresponding sensitivities from our 4 highest sites  
710 (1190-2540 m) were AS = -18.2 cm/°C, RS = -13%/°C (cf. Fig. 6).

711 BENISTON et al. (2003a) used meteorological and snow depth measurements from 18 Swiss  
712 stations in the elevation range 317-2500 m to derive an empirical response surface to  
713 predict long-term mean  $N_d(S > 0 \text{ cm})$  in subperiod  $P_0$  as a function of December to  
714 February mean temperature and precipitation. They considered a 2 °C warming and they  
715 state for the sites Arosa at 1847 m and Säntis at 2500 m AS = -25 d/°C (both sites), RS =  
716 -22 %/°C (Arosa) and -9 %/°C (Säntis). Our results for Davos (1590 m) and  
717 Weissfluhjoch (2540 m) were AS = -14.6 d/°C and -15 d/°C and RS = -11 %/°C and -6.4  
718 %/°C, respectively (cf. Fig. 7, left).

719 BENISTON et al. (2003b) analyzed the same empirical data set, and for  $N_d(S > 0 \text{ cm})$  and  
720 subperiod  $P_0$  they suggested for all elevations an AS range between -15 d/°C and -20 d/°C.  
721 Our corresponding estimate was AS = -16.6 d/°C (Table 7).



722

723 **Figure 10:** Comparison of estimated sensitivities of snow cover statistics with the results  
724 from earlier Swiss studies. Top: Absolute sensitivities (AS); bottom: Relative sensitivities  
725 (RS).  $N_d(S \geq h)$ : long-term mean number of days at which snow depth exceeds h. All  
726 statistics refer to subperiod  $P_0$ , except for the rightmost  $N_d$  statistic which refers to subperiod  
727  $P_2$ . NA: data not available. Bult 92: BULTOT et al. (1992); Bult 94: BULTOT et al. (1994);  
728 Beni 03a: BENISTON et al. (2003a); Beni 03b: BENISTON et al. (2003b); Schu 97:  
729 SCHULLA (1997); Stad 98: STADLER et al. (1998); Ehrl 98: EHRLER (1998). Note, the  
730 earlier studies considered in most cases other regions, locations, climatic baselines and/or  
731 climate scenarios than the ones used in this study. Comparison was done using the most  
732 similar results available from the present work. For details see text.

733 Finally, WIELKE et al. (2004) investigated the sensitivity of snow cover at 59 Swiss  
734 stations to interannual variations in European winter mean temperature ( $T_{winE}$ ). They  
735 considered  $N_d(S \geq 5 \text{ cm})$  for winter (December to February) and spring (March to May),  
736 and they defined sensitivity by the maximum slope of a fitted logistic curve  $N_d = f(T_{winE})$   
737 (cf. Figs. 7 and 9). They found for winter AS = -27.3 d/°C and for spring AS = -35.9 d/°C.

738 The results of our comparisons are summarized in Fig. 10. The study by WIELKE et al.  
 739 (2004) was not included in this figure because of the very different definition of sensitivity  
 740 in this work (use of European temperature  $T_{winE}$ ) as compared to all other studies (use of  
 741 regional or local temperatures). This issue is discussed in more detail in Section 4.1.2.

742 From Fig. 10 can be seen that our sensitivity estimates were generally lower than those  
 743 obtained in earlier studies. The found differences were somewhat smaller for long-term  
 744 mean snow depth (Fig. 10, right) as compared to the  $N_d$  statistics (left) and for the RS  
 745 (bottom) as compared to the AS (top) statistics.

### 746 3.5 Comparison with Other Regions

747 Various studies have addressed the sensitivity of snow cover in other regions. Below we  
 748 discuss a selection of quantitative results known to us. We focus on the AS of the long-  
 749 term mean number of days with snow lying on the ground,  $N_d(S > 0 \text{ cm})$  during subperiod  
 750  $P_o$  (here simply abbreviated as  $N_d$ ) since this was the most frequently reported statistic.

751 For Austria KOCH & RUDEL (1990) estimated based on a statistical analysis of measured  
 752 temperatures and snow cover data AS = 25 d/°C. HANTEL et al. (2000) applied a much  
 753 more sophisticated analysis technique to an extensive empirical data base from the same  
 754 region and obtained for winter (for spring) AS = 31 d/°C (42 d/°C).

755 For the French Alps MARTIN et al. (1994) investigated the sensitivity of the coupled  
 756 SAFRAN/CROCUS meteorological-analysis and multi-layer snow models to changed  
 757 temperature and radiation conditions as derived from a "double CO<sub>2</sub>" GCM experiment.  
 758 Their results suggested for  $N_d$  at 1500 m (at 3000 m) AS = 17-22 d/°C (11-17 d/°C).

759 MARTIN et al. (1997) combined the same modelling system with a spatial downscaling  
 760 procedure and considered climatic changes as simulated by two further GCMs. For areal  
 761 mean  $N_d$  in the Mont-Blanc region in the north-eastern part of the French Alps they  
 762 reported (their Fig. 8 and Table 4) at 1500 m AS = -29 d/°C (RS = -19.4 %/°C). For the  
 763 Mercantour massif in the south-eastern part of the French Alps they obtained for the  
 764 same elevation AS = -28.3 d/°C (RS = -45.4 %/°C).

765 The sensitivities of the Estonian and the Scottish snow cover have been assessed based on  
 766 the analysis of observed snow cover-temperature covariations. JAAGUS (1997) found for  
 767 the West-Estonian archipelago ( $T_{win} < -1 \text{ °C}$ ) AS = -11 to -12 d/°C, and for the cooler  
 768 ( $T_{win} = -3 \text{ to } -5 \text{ °C}$ ) inland and eastern parts of Estonia AS = -7 to -10 d/°C. HARRISON  
 769 et al. (2001) reported for Scotland an average value of AS = -9 d/°C.

770 Finally, the sensitivity of south-east Australian snow cover has been studied by  
 771 WHETTON et al. (1996). On average over 8 locations in the elevation range 1564 m to 2228  
 772 m their results (their Table III) suggest for temperature changes of up to 2 °C and  
 773 precipitation changes between -10% and +20% AS = -32.1 d/°C (RS: -38 %/°C) (Note,  
 774 these numbers do not consider their "year 2070 worst-case" scenario because under this  
 775 assumption they obtained for most sites no snow cover at all). As was the case in the  
 776 present study their sensitivities tended to decrease with elevation. However, quite  
 777 differently from our results (Fig. 6), they concluded that under a general warming  
 778 precipitation changes up to 20% would have only a small impact on the snow cover  
 779 duration.

## 4. DISCUSSION

### 4.1 Climatic Sensitivity of the Swiss Snow Cover

Our results (Figs. 6 to 8, Tables 7 to 9) indicate that a mean temperature increase in the order of 2 °C to 4 °C would lead to a general decrease in the average duration and depth of Swiss snow cover, at least up to elevations of ~2500 m. This decrease would show marked regional and seasonal variations, and it would be significantly modulated by possible changes in precipitation (Figs. 6, 7 and 9).

The largest sensitivities to a warming (Figs. 6 and 9) were generally obtained at the three lower-elevation sites. This can be explained by the fact that at these sites the present-day winter mean temperature is close to, or only slightly above the freezing point (cf. Table 1).

The found high sensitivity at lower elevations is consistent with the results from several observational studies: Based on an analysis of data from 12 Swiss locations (elevation range 276-2540 m) for the period 1980-1994 BENISTON (1997) found a strong increase in relative variability (defined as the standard deviation divided by the mean) of  $N_d(S \geq h)$  with decreasing elevation and increasing  $h$ ; he thus concluded that snow cover at sites below 1500 m is increasingly sensitive to the occurrence of warm winters. BENISTON et al. (2003b) also studied possible changes in long-term mean Swiss total snow volume due to a wintertime warming by +2 and +4 °C using data from 18 Swiss stations and they also found a decreasing sensitivity with elevation. LATERNSE & SCHNEEBELI (2003) analyzed snow cover variations at 140 Swiss stations for the period 1931-1999. For the particularly warm, last two decades of the 20th century they detected a general decrease in winter mean snow depths, which increased with decreasing elevation. A similar result was also reported by SCHERRER et al. (2004). Finally, WIELKE et al. (2004) estimated that the elevation of maximum sensitivity for the Swiss snow cover is 580 m in winter and 1370 m in spring.

Our results demonstrated a stronger sensitivity of the snow cover to a warming during spring as compared to early winter (Fig. 6). This finding suggests that the effects of a general temperature increase are dampened by the seasonal cooling at the beginning of the snow season, but that they are amplified by the seasonal warming at the end of the snow season.

The found seasonal variation in the snow cover's sensitivity is also in line with earlier studies: FÖHN (1990) suggested that under a 3 °C temperature increase (and given no major changes in precipitation) the snow cover at an elevation of ~1500 m would build up later, at the first half of December, and that it would disappear already by the end of March. Our results for Montana and Davos (Fig. 6) are remarkably consistent with his assessment. LATERNSE & SCHNEEBELI (2003) found in their analysis of long-term Swiss snow measurements a weak trend towards a later build up of snow cover at mid elevations (1000-1600 m) and a general trend towards earlier melting of the snow cover. This result is again supported by the empirical study of WIELKE et al. (2004), who found smaller sensitivities for winter as opposed to spring.

The higher sensitivity during springtime has also been found in the modelling studies by EHRLER (1998) for the Upper Rhine basin; by BENISTON et al. (2003b) for the site Säntis (2500 m), based on experiments with the GRENBLS surface energy balance model; and by JASPER et al. (2004), who applied the WaSiM-ETH model in the Thur and Ticino catchments to a range of climate change scenarios. The latter study reported a delay in the

825 onset of the snow season by 1 to 3 weeks, and an earlier begin of snow-free conditions at  
 826 1000 m by 5 to 8 weeks, depending on scenario. They attributed the strong response  
 827 during the melting period to the seasonal warming pattern in their scenarios. Our  
 828 simulations using seasonally uniform changes in temperature (Fig. 6) suggest, however,  
 829 that the main reason for this response is the amplification of the climate change signal by  
 830 the seasonal warming during springtime.

831 Fig. 6 demonstrated that in our study region a decrease (an increase) in average  
 832 precipitation would reinforce (counteract) the simulated negative effects of a warming on  
 833 the snow cover (Fig. 6). This precipitation effect has also been noted by BENISTON et al.  
 834 (2003a, 2003b), who found a smaller temperature sensitivity of Swiss snow volume for  
 835 wetter-than-average winters as compared to dry winters.

836 Our results suggest that the compensating effect of a precipitation increase is smaller at  
 837 lower elevations and during spring, as compared to higher elevations and during winter  
 838 (Fig. 6). This appears plausible, since it can be expected that with decreasing average  
 839 temperatures an increasing proportion of precipitation will fall as snow (cf. Eqs. 5, Table  
 840 2). Accordingly, at the warmer, low-elevation sites the precipitation increases that were  
 841 specified in the "warm/wet" CCC-scenario (Fig. 5) did not help much to alleviate the  
 842 stronger decay of the snow cover as compared to the "cool/dry" ECHAM scenario.  
 843 However, at the mid-elevation site Davos both scenarios gave similar changes, and at the  
 844 site Weissfluhjoch the wetter CCC scenario even yielded a smaller decrease as compared to  
 845 the ECHAM scenario (Fig. 6, right).

846 This increasing importance of changes in precipitation with increasing elevation has also  
 847 been reported by MARTIN et al. (1997) for the French Alps and by EHRLER (1998, pp.  
 848 90-91) for Switzerland. He found that for October through March (his definition of the  
 849 winter season) the effects of a 2 °C temperature increase on the snow cover could be  
 850 compensated by a 20% precipitation increase above an elevation of ca. 2100 m. For a 3 °C  
 851 warming he suggested a compensation point between 2100 and 2400 m. Our findings agree  
 852 quite well with his estimates (see Fig. 6, site Weissfluhjoch).

## 853 4.2 Quantitative Comparison of Sensitivities

854 In spite of the general qualitative agreement with the results from the earlier Swiss studies,  
 855 the quantitative comparisons (Fig. 10) showed that our simulations gave generally lower  
 856 sensitivity values than reported previously. We believe that several different factors have  
 857 contributed to this result:

858 1. Sampling uncertainty: Most earlier *model-based* studies have considered only a limited  
 859 number of years (ten or so). Given the large temporal variability of the Swiss snow cover  
 860 (LATERNER & SCHNEEBELI 2003; Figs. 4 and 8) it seems therefore possible that at least  
 861 part of the deviations is a statistical artefact. However, this explanation might not hold  
 862 when comparing with earlier *empirical* studies, since these have typically used larger data  
 863 samples.

864 Particularly large deviations were obtained as compared to the empirical study by  
 865 BENISTON et al. (2003a) (Fig. 10, top). However, to our understanding, the sensitivity  
 866 estimates quoted in this study were extracted from a simple response surface graph, and  
 867 this rough procedure would translate into a large estimation variance. We therefore believe  
 868 that the found differences (Fig. 10) are not statistically significant. BENISTON et al.  
 869 (2003b) reported later for  $N_d(S > 0 \text{ cm})$  a sensitivity range of -15 d/°C to -20 d/°C. This

870 result appears to have been inferred from a more robust statistical analysis and it is in  
871 much better agreement with our average estimate of  $-16.6 \text{ d}/^\circ\text{C}$ .

872 2. Limited comparability of studies: The various studies considered different regions,  
873 climatic baseline periods, or climate scenarios. Moreover, they employed alternative  
874 definitions of the winter mean temperature, of the snow depth thresholds defining a day  
875 with snow lying on the ground, or of the seasonal time windows used to compute the  
876 snow cover statistics. Note also that in most earlier studies snow depth was derived from  
877 the total water equivalent of the snow cover by assuming a constant snow density (e.g.,  
878 BULTOT et al. 1994, SCHULLA 1997), whereas in this study snow depth was modelled  
879 explicitly. The highly non-linear equations used to describe the settling of the snow cover  
880 (Eqs. 7, 8) suggest the potential for major deviations between the two approaches.

881 The fact that WIELKE et al. (2004) obtained much higher AS values (between  $-27 \text{ d}/^\circ\text{C}$  to -  
882  $36 \text{ d}/^\circ\text{C}$ ) as compared to all other Swiss studies (including this one, see Fig. 10) seems to  
883 have been caused by such methodical differences. The main reason probably lies in their  
884 use of European mean temperatures ( $T_{\text{winE}}$ , sector  $5\text{-}25^\circ\text{E}$  and  $42.5\text{-}52.5^\circ\text{N}$ ) to define the  
885 sensitivity, whereas all other Swiss studies used regional or local  $T_{\text{win}}$  variables. Since all  
886 sensitivity estimates are based on regressing a snow cover statistic on a temperature  
887 variable (Eq. 10, Fig. 7), the sensitivities can be expected to scale in a first approximation  
888 inversely with the standard deviation (SD) of the temperature variable. For the analysis  
889 period 1961-1990 considered by WIELKE et al. (2004) we found  $\text{SD}(T_{\text{winS}})/\text{SD}(T_{\text{winE}}) =$   
890  $1.32$ , where  $T_{\text{winS}}$  stands for the Swiss areal mean winter temperature (analyses not  
891 shown). Hence, the use of  $T_{\text{winE}}$  probably yields higher sensitivities by ca. 30%. Even  
892 bigger differences in sensitivity can be expected to occur when local temperatures are used,  
893 which show even larger variabilities than  $T_{\text{winE}}$  and  $T_{\text{winS}}$  (not shown).

894 A further reason probably relates to the use of a 5 cm snow depth threshold ( $h$ ) by  
895 WIELKE et al. (2004). When considering subperiod  $P_2$  (which is the most similar seasonal  
896 time window available from our study as compared to the winter definition used by  
897 WIELKE et al. 2004) it can be seen from our Table 7 that both, AS as well as RS, tend to  
898 increase with increasing  $h$  (at least for  $h < 20 \text{ cm}$ ). Hence, alternative definitions of  $h$  could  
899 also contribute to the higher values obtained by WIELKE et al. (2004) as compared to our  
900 study.

901 3. Model limitations: It is remarkable that our results differ quite strongly from those  
902 obtained from simulations with distributed (SCHULLA 1997, JASPER et al. 2004) or semi-  
903 distributed (BULTOT et al. 1992, 1994; EHRLER 1998) models, whereas they agree quite  
904 well with those obtained from another site-specific simulation approach (STADLER et al.  
905 1998; see Fig. 10). We therefore surmise that the (semi-)distributed models tend to  
906 systematically overestimate the true sensitivity of the *local* snow cover. We speculate  
907 that this is due to discretisation effects, and/or because these models were tuned to  
908 simulate hydrology and snow cover at a relatively coarse spatial resolution, e.g. for  
909 gridboxes of size  $0.25 \text{ km}^2$  (SCHULLA 1997) or for different elevation zones (BULTOT et al.  
910 1992, 1994; EHRLER 1998).

911 4. Data Problems: Some of the found differences may also have been caused by errors in  
912 the used input data sets. One important error source is the underestimation of solid  
913 precipitation due to rain gauge undercatch (e.g. SEVRUK 1985), a factor that has been  
914 treated differently in the various modelling studies. Another problem relates to possible  
915 inconsistencies in the weather data used to tune or drive the models. For instance, at our

916 site Weissfluhjoch meteorological and snow data were not measured at exactly the same  
917 locations, and this may have caused some systematic deviations in our simulations.

918 Our quantitative comparison with results from other world regions (Section 3.5)  
919 considered only a limited sample of studies. Nevertheless, the comparison clearly suggests  
920 that beyond the general response patterns found in this and earlier studies (e.g., maximum  
921 sensitivity in situations where long-term mean temperatures are close to the freezing point;  
922 compensation of a warming by possible increases in precipitation) the currently available  
923 quantitative estimates for the sensitivity of the snow cover show substantial variation  
924 across regions. The only apparent pattern appears to be a somewhat lower sensitivity  
925 with increasing latitude (Scotland, Estonia) as compared to the European Alpine region.  
926 Yet, it is again not clear in as far these differences are real, since the various methodical  
927 problems discussed above with regard to the Swiss studies apply equally to any  
928 comparisons between regions.

929 A better explanation of the found differences between studies would require a much more  
930 rigorous intercomparison of data sets, analysis procedures, and models. This was however  
931 beyond the scope of this work.

### 932 **4.3 Critique of Method**

933 The proposed method (Fig. 1) has two salient features: (i) it employs a modular, linear  
934 "end-to-end" approach that deals separately with the spatial and the temporal variability  
935 of regional climate, and (ii) it makes extensive use of empirical data.

936 Feature (i) has the advantage that the individual steps can be flexibly used, tested and  
937 improved independently from each other. For example, our procedure enabled us to study  
938 sensitivities based on arbitrary assumptions as well as on GCM-derived local climatic  
939 scenarios (Figs. 5 and 6). Alternative scenarios could easily have been introduced based on  
940 simulations with other GCMs, or regional climate models (RegCMs), or any combination  
941 of climate scenario construction approaches (MEARNS et al. 2001).

942 The use of empirical data (ii) helped to increase the realism of our simulations, albeit at the  
943 cost of introducing problems related to data availability, the robustness of the used  
944 statistical relationships, and their stationarity under a changing climate.

945 These problems are probably less acute with regard to the temporal downscaling  
946 procedure and the snow model, where it was demonstrated that 5 and 14 years of data for  
947 model tuning, respectively, enable accurate simulation of the snow cover's variability over  
948 a wide range of time scales (Fig. 4, Tables 4 and 5). Our snow cover simulations tended  
949 however to underestimate long-term mean daily snow depths (Fig. 3, Table 4). This  
950 probably relates to the fact that the used version (v2.5b) of the WeathGen software  
951 implements a step-like change in the expected values of the daily temperature variables  
952 between months. This resulted into anomalously warm temperatures, and hence reduced  
953 snow accumulation, in the second halves of the early winter months. Newer versions of  
954 the WeathGen software that employ a smoother representation of temperature variables'  
955 annual cycle would probably allow to further improve our results.

956 Several improvements seem also possible with regard to the spatial downscaling  
957 procedure, for instance by using additional large-scale predictor fields and/or by adopting a  
958 daily time step (e.g., BUIHAND et al. 2004). Note, however, that our overall method is  
959 less sensitive to shortcomings of the spatial downscaling step as compared to other

960 approaches that make direct use of downscaled weather data (e.g., MARTIN et al. 1997).  
961 This is because we use spatial downscaling only in order to estimate changes in long-term  
962 mean climate (Fig. 5, Table 6; see also VON STORCH 1999), whereas the local high-  
963 frequency weather variations are simulated accurately by means of temporal downscaling.  
964 Nevertheless, the scenario changes obtained for poorly downscaled variables (such as the  
965 monthly standard deviations of daily temperatures, see GYALISTRAS et al. 1994) can not  
966 be trusted much. Sensitivity analyses to test the importance of possible changes in these  
967 variables could be easily carried out with our method.

968 Note that the temporal downscaling procedure greatly helped to improve the robustness of  
969 our sensitivity estimates. Firstly, it enabled us to accurately simulate local snow cover  
970 statistics based on a limited number of monthly weather inputs (Figs 3 and 4, Tables 4 and  
971 5). Purely statistical approaches that attempt to predict snow cover statistics from  
972 monthly (e.g., BREILING & CHARAMZA 1999) or seasonal (e.g., SCHERRER et al. 2004)  
973 mean temperature and precipitation typically yield  $r^2$  values below 50%. Our model chain  
974 gave clearly better results (Table 4). Secondly, by providing a large number of possible  
975 daily weather developments the temporal downscaling approach enabled a robust  
976 estimation of the expected values of daily (Figs 3 and 6) or annual (Fig. 4) snow cover  
977 variables conditional on monthly weather. And finally, thanks to its computational  
978 efficiency, it allowed us to easily carry out thousands of simulations in order to explore a  
979 wide range of possible changes in climate (Figs 6 to 9). This contrasts with earlier studies  
980 (see Section 3.4) that have typically explored but a limited number of changes in climate  
981 parameters and annual weather courses.

982 Our method compares favourably with similar model-based approaches: WHETTON et al.  
983 (1996) have also used monthly weather data to drive a local snow model. However,  
984 different from our study their model employed but a monthly time step. They reported  
985 for  $N_d(S > 0 \text{ cm})$  a root mean square error of 30 days. The corresponding value from our  
986 simulations was 11 days (average over the four lowest locations for period P<sub>1</sub>; cf. Table  
987 4). SCOTT et al. (2002, 2003) combined the LARS daily weather generator (SEMENOV et  
988 al. 1998) with a daily snow model. They found that this model did not simulate individual  
989 years very reliably (SCOTT et al. 2002, p.26). Moreover, their weather generator is known  
990 to systematically underestimate the interannual variability of monthly weather variables  
991 (MAVROMATIS & HANSEN 2001). This systematic error is likely to further distort the  
992 long-term snow cover statistics obtained in their simulations. Therefore we believe that  
993 our method gives more accurate results.

994 A major disadvantage of our simulation approach is that it does not consider many  
995 relevant processes and feedbacks, such as radiation and slope-aspect effects, the  
996 redistribution of snow by wind, the lowering of the freezing level in narrow valleys during  
997 heavy precipitation events, regional atmospheric circulations, or the albedo-temperature  
998 feedback. A further limitation arises from the fact that each site is simulated  
999 independently, such that the resulting scenarios are spatially not consistent if one wishes  
1000 to consider individual years across locations.

1001 Some of these problems could be solved by using physically based point simulation  
1002 models (e.g. ESSERY et al. 1999), spatially distributed models (see Section 3.4), or even  
1003 regional climate models (e.g., KLEINN 2002, LEUNG et al. 2004). However, to our  
1004 knowledge, the feasibility (parameters, weather inputs) and capability of these modelling  
1005 approaches to accurately simulate the temporal variability of snow cover over longer time  
1006 scales (Fig. 4, Table 4) has yet to be demonstrated.

## 5. CONCLUSIONS

This work shows that by combining a temporal downscaling procedure with a conceptual snow model it is possible to accurately simulate the seasonal to decadal-scale variability of local snow cover based on only eight monthly variables related to temperature and precipitation. The mean and the interannual variability of several Swiss snow cover indices of importance to the winter tourism industry is well reproduced (mean relative errors < 15%,  $r = 0.7$  to  $0.9$ ). Model performance generally decreases the shorter the seasonal time window used to define a snow cover statistic.

The Swiss snow cover below 1600 m is primarily governed by temperature, but precipitation becomes increasingly important with elevation. Temperature sensitivity increases with decreasing elevation, it is larger during spring as compared to earlier in the snow season, and it shows substantial inter-site variations. At elevations above 2500 m an increase in winter mean precipitation by 20% could offset the effects of a 4 °C warming, at least for the time from October through March.

Different snow cover statistics show widely varying sensitivities. However, the sensitivities depend systematically on the choice of the snow depth threshold and seasonal time window. Climate change will strongly affect the higher-order moments (variance, skewness) of annual snow depth indices. Frequencies of years with specific snow cover characteristics (e.g., suitability of natural snow conditions for downhill skiing) can be expected to change non-linearly with a gradual change in climate.

The simulated snow cover responses appear physically plausible and are generally consistent with earlier observational and modelling studies for our study area. Our site-specific simulation approach gives somewhat lower sensitivities than have been reported earlier for the Swiss region. Quantitative comparisons between studies are however currently hampered by major methodical problems. Rigorous, systematic intercomparisons are needed in order to better understand the obtained variations in the sensitivity of local snow cover between different studies or regions.

On average over all scenarios and sites investigated the long-term mean number of days with snow lying on the ground between September 1st and July 31st was found to decrease by 17 d per °C change in the winter half-year (November-April) mean temperature. The number of days with snow depth exceeding 30 cm in the main skiing season (December 1st through April 15<sup>th</sup>) was found to decrease by on average 14 d/°C. The relative frequency of years with at least 100 days with snow depth exceeding the 30 cm threshold during the same period was found to decrease by on average 12.5%/°C.

The comparatively low input requirements of our method enable reliable long-term reconstructions of snow cover statistics from monthly weather data, they justify the use of parsimonious climatic scenarios, and they contribute to enhancing the robustness of future snow cover projections. Moreover, our method was shown to be more accurate than alternative methods proposed in earlier studies. Its adaptation to alternative needs by climate impact analysts, or other radiative forcing scenarios, climate models and regions appears straight-forward.

1048 **Acknowledgements.**

1049 Research of DG and MS was supported by the EU-project "Modelling of the Impact of  
 1050 Climate Extremes" (MICE, EVK20CT2001-0018). Particular thanks go to B. Abegg and  
 1051 R. Bürki for many inspiring discussions. The provision of snow and weather data by the  
 1052 Swiss Federal Institute for Snow and Avalanche Research Davos (SLF) and MeteoSwiss is  
 1053 gratefully acknowledged.

1054 **6. REFERENCES**

- 1055 Abegg, B., 1996: Klimaänderung und Tourismus: Klimafolgenforschung am Beispiel des Wintertourismus  
 1056 in den Schweizer Alpen (Climate change and tourism: climate impact research exemplified by  
 1057 winter tourism in the Swiss Alps). vdf, Hochschulverlag AG an der ETH Zürich, 222 pp.
- 1058 Baumgartner, M. and A. Rango, 1995: A microcomputer-based alpine snow-cover analysis system  
 1059 (ASCAS). *Photogrammetric Engineering and Remote Sensing*, **61**, 1475-1486.
- 1060 Beckmann, B.-R. and T. A. Buishand, 2002: Statistical downscaling relationships for precipitation in the  
 1061 Netherlands and North Germany. *International Journal of Climatology*, **22**, 15-32.
- 1062 Beniston, M., 1997: Variations of snow depth and duration in the Swiss Alps over the last 50 years: links  
 1063 to changes in large-scale climatic forcings. *Climatic Change*, **36**, 281-300.
- 1064 Beniston, M., F. Keller, and S. Goyette, 2003: Snow pack in the Swiss Alps under changing climatic  
 1065 conditions: an empirical approach for climate impacts studies.  
 1066 *Theoretical and Applied Climatology*, **74**, 19-31.
- 1067 Beniston, M., F. Keller, B. Koffi, and S. Goyette, 2003: Estimates of snow accumulation and volume in  
 1068 the Swiss Alps under changing climatic conditions. *Theoretical and Applied Climatology*, **76**, 125-  
 1069 140.
- 1070 Boer, G. J., N. A. McFarlane, and M. Lazare, 1992: Greenhouse gas-induced climate change simulated with  
 1071 the CCC second-generation general circulation model. *Journal of Climate*, **5**, 1045-1077.
- 1072 Braun, L. N. and C. B. Renner, 1992: Application of a conceptual runoff model in different physiographic  
 1073 regions of Switzerland. *Hydrological sciences journal*, **37**, 217-231.
- 1074 Braun, L. N., E. Brun, Y. Durand, E. Martin, and P. Tourasse, 1994: Simulation of discharge using  
 1075 different methods of meteorological data distribution, basin discretization and snow modelling.  
 1076 *Nordic Hydrology*, **25**, 129-144.
- 1077 Breiling, M. and P. Charamza, 1999: The impact of global warming on winter tourism and skiing: a  
 1078 regionalised model for Austrian snow conditions. *Regional Environmental Change*, **1**, 4-14.
- 1079 Briffa, K. R. and P. D. Jones, 1993: Global surface air temperature variations during the twentieth century:  
 1080 Part 2, implications for large-scale high-frequency paleoclimatic studies. *The Holocene*, **3**, 77-88.
- 1081 Buishand, T.A., Shabalova, M.V. and Brandsma, T., 2004: On the choice of the temporal aggregation  
 1082 level for statistical downscaling of precipitation. *Journal of Climate*, **17**, 1816-1827.
- 1083 Bultot, F., D. Gellens, M. Spreafico, and B. Schädler, 1992: Repercussions of a CO2 doubling on the  
 1084 water balance - a case study in Switzerland. *Journal of Hydrology*, **137**, 199-208.
- 1085 Bultot, F., D. Gellens, B. Schädler, and M. Spreafico, 1994: Effects of climate change on snow  
 1086 accumulation and melting in the Broye catchment (Switzerland). *Climatic Change*, **28**, 339-363.
- 1087 Bürki, R., 2000: Klimaänderung und Anpassungsprozesse im Wintertourismus (Climate change and  
 1088 adaptation processes in winter tourism). Ostschweizerische Geographische Gesellschaft, St. Gallen,  
 1089 206 pp.
- 1090 Charles, S. P., B. C. Bates, P. H. Whetton, and J. P. Hughes, 1999: Validation of downscaling models for  
 1091 changed climate conditions: case study of southwestern Australia. *Climate Research*, **12**, 1-14.

- 1092 Cubasch, U., K. Hasselmann, H. Höck, E. Maier-Reimer, U. Mikolajewicz, B. D. Santer, and R. Sausen,  
1093 1992: Time-dependent greenhouse warming computations with a coupled ocean-atmosphere model.  
1094 *Climate Dynamics*, **8**, 55-69.
- 1095 Cubasch, U., G. A. Meehl, G. J. Boer, R. J. Stouffer, M. Dix, A. Noda, C. A. Senior, S. Raper, and K. S.  
1096 Yap, 2001: Projections of future climate change. *Climate change 2001: The scientific basis.*  
1097 *Contribution of working group I to the third assessment report of the Intergovernmental Panel on*  
1098 *Climate Change*, J. T. Houghton, Y. Ding, D. J. Griggs, M. Noguer, P. J. van der Linden, X.  
1099 Dai, K. Maskell, and C. A. Johnson, Eds., Cambridge University Press, 525-582.
- 1100 Ehrler, C., 1998: Klimaänderung und alpine Schneedecke - Auswirkungen auf das Abflussregime am  
1101 Beispiel des Einzugsgebiets Rhein-Felsberg (Climate change and the alpine snow cover -  
1102 Consequences for the runoff regime using the Rhein-Felsberg catchment as an example). vdf  
1103 Hochschulverlag an der ETH, 134 pp.
- 1104 Etchevers, P., Martin, E., Brown, R., Fierz, C., Lejeune, Y., Bazile, E., Boone, A., Dai, Y.-J., Essery, R.,  
1105 Fernandez, A., Gusev, Y., Jordan, R., Koren, V., Kowalczyk, E., Nasonova, N.O., Pyles, R.D.,  
1106 Schlosser, A., Shmakin, A.B., Smirnova, T.G., Strasser, U., Verseghy, D., Yamazaki, T. & Yan,  
1107 Z.-L. (2004). Validation of the energy budget of an alpine snowpack simulated by several snow  
1108 models (SNOWMIP project). *Ann. Glaciol.* **38**, 150-158.
- 1109 Essery, R., E. Martin, H. Douville, A. Fernandez, and E. Brun, 1999: A comparison of four snow models  
1110 using observations from an alpine site. *Climate Dynamics*, **15**, 583-593.
- 1111 Fischlin, A. and D. Gyalistras, 1997: Assessing impacts of climatic change on forests in the Alps.  
1112 *Global Ecology and Biogeography Letters*, **6**, 19-37.
- 1113 Föhn, P., 1990: Schnee und Lawinen (Snow and avalanches). *Schnee, Eis und Wasser der Alpen in einer*  
1114 *wärmeren Atmosphäre*, Zurich, Versuchsanstalt für Wasserbau, Hydrologie und Glaziologie der  
1115 ETH Zürich, 33-48.
- 1116 Gates, W. L., A. Henderson-Sellers, G. J. Boer, C. K. Folland, A. Kitoh, B. J. McAvaney, F. Semazzi, N.  
1117 Smith, A. J. Weaver, and Q.-C. Zeng, 1996: Climate models - evaluation. *Climate Change 1995:*  
1118 *The Science of Climate Change. Contribution of Working Group I to the Second Assessment*  
1119 *Report of the Intergovernmental Panel on Climate Change*, J. T. Houghton, L. G. Meira Filho, B.  
1120 A. Callander, N. Harris, A. Kattenberg, and K. Maskell, Eds., Cambridge University Press, 229-  
1121 284.
- 1122 Giorgi, F., J. W. Hurrell, M. R. Marinucci, and M. Beniston, 1997: Elevation dependency of the surface  
1123 climate change signal: a model study. *Journal of Climate*, **10**, 288-296.
- 1124 Gyalistras, D., Fischlin, A. & Riedo, M. 1997. Herleitung stündlicher Wetterszenarien unter zukünftigen  
1125 Klimabedingungen. In: Fuhrer, J. (ed.), *Klimaänderung und Grünland - eine Modellstudie über*  
1126 *die Auswirkungen einer Klimaänderung auf das Dauergrünland in der Schweiz*. vdf,  
1127 Hochschulverlag AG an der ETH Zürich, pp. 207-276.
- 1128 Gyalistras, D. and A. Fischlin, 1999: Towards a general method to construct regional climatic scenarios for  
1129 model-based impacts assessments. *Petermanns geographische Mitteilungen*, **143**, 251-264.
- 1130 Gyalistras, D., H. von Storch, A. Fischlin, and M. Beniston, 1994: Linking GCM-simulated climatic  
1131 changes to ecosystem models: case studies of statistical downscaling in the Alps.  
1132 *Climate Research*, **4**, 167-189.
- 1133 Gyalistras, D., C. Schär, H. C. Davies, and H. Wanner, 1998: Future Alpine climate. *Views from the Alps:*  
1134 *regional perspectives on climate change*, P. Cebon, U. Dahinden, H. C. Davies, D. Imboden, and  
1135 C. Jäger, Eds., MIT Press, 171-223.
- 1136 Hantel, M., M. Ehrendorfer, and A. Haslinger, 2000: Climate sensitivity of snow cover duration in Austria.  
1137 *International Journal of Climatology*, **20**, 615-640.
- 1138 Harrison, J., Winterbottom, S. & Johnson, R., 2001: Climate change and changing snowfall patterns in  
1139 Scotland. The Scottish Executive Central Research Unit, Edinburgh, 48pp.
- 1140 Jaagus, J., 1997: The impact of climate change on the snow cover pattern in Estonia. *Climatic Change*, **36**,  
1141 65-77.
- 1142 Jasper, K., Calanca, P., Gyalistras, D. & Fuhrer, J., 2004: Differential impacts of climate change on the  
1143 hydrology of two alpine river basins. *Clim. Res.*, **26**, 113-129.

- 1144 Jones, P. D. and K. R. Briffa, 1992: Global surface air temperature variations during the twentieth century:  
1145 Part I, spatial, temporal and seasonal details. *The Holocene*, **2**, 165-179.
- 1146 Jones, P.D. & Moberg, A. (2003). Hemispheric and large-scale surface air temperature variations: An  
1147 extensive revision and an update to 2001. *J. Clim.*, **16**, 206–223.
- 1148 Kleinn, J., 2002: Climate change and runoff statistics in the Rhine Basin: a process study with a coupled  
1149 climate-runoff model, Swiss Federal Institute of Technology (ETH), 114.
- 1150 Koch, E. and E. Rudel, 1990: Mögliche Auswirkungen eines verstärkten Treibhauseffektes auf die  
1151 Schneeverhältnisse in Österreich (Possible consequences of an enhanced greenhouse effect on snow  
1152 conditions in Austria). *Wetter und Leben*, **45**, 137-153.
- 1153 Laternser, M. and M. Schneebeli, 2003: Long-term snow climate trends of the Swiss Alps (1931-99).  
1154 *International Journal of Climatology*, **23**, 733-750.
- 1155 Leung, L. R., Y. Qian, X. Bian, W. M. Washington, J. Han, and J. O. Roads, 2004: Mid-century  
1156 ensemble regional climate change scenarios for the western united states. *Climatic Change*, **62**, 75-  
1157 113.
- 1158 Martin, E., Brun, E. & Durand, Y., 1994: Sensitivity of the French Alps snow cover to the variation of  
1159 climatic variables. *Ann. Geophys.*, **12**, 469-477.
- 1160 Martin, E., B. Timbal, and E. Brun, 1997: Downscaling of general circulation model outputs: simulation  
1161 of the snow climatology of the French Alps and sensitivity to climate change. *Climate Dynamics*,  
1162 **13**, 45-56.
- 1163 Martinec, J., 1977: Expected snow loads on structures from incomplete hydrological data.  
1164 *The Journal of Glaciology*, **19**, 185-195.
- 1165 Mavromatis, T. & Hansen, J.W., 2001: Interannual variability characteristics and simulated crop response of  
1166 four stochastic weather generators. *Agric. For. Meteorol.* **109**, 283-296.
- 1167 McFarlane, N. A., G. J. Boer, J.-P. Blanchet, and M. Lazare, 1992: The Canadian Climate Centre second-  
1168 generation general circulation model and its equilibrium climate. *Journal of Climate*, **5**, 1013-  
1169 1044.
- 1170 Mearns, L. O., M. Hulme, T. R. Carter, R. Leemans, M. Lal, and P. Whetton, 2001: Climate scenario  
1171 development. *Climate change 2001: The scientific basis. Contribution of working group I to the*  
1172 *third assessment report of the Intergovernmental Panel on Climate Change*, J. T. Houghton, Y.  
1173 Ding, D. J. Griggs, M. Noguer, P. J. van der Linden, X. Dai, K. Maskell, and C. A. Johnson,  
1174 Eds., Cambridge University Press, 739-768.
- 1175 Monro, J. C., 1971: Direct search optimization in mathematical modelling and a watershed application.  
1176 NOAA Technical Memorandum NWS HYDRO, 52 pp.
- 1177 Riedo, M., D. Gyalistras, A. Fischlin, and J. Fuhrer, 1999: Using an ecosystem model linked to GCM-  
1178 derived local weather scenarios to analyse effects of climate change and elevated CO<sub>2</sub> on dry matter  
1179 production and partitioning, and water use in temperate managed grasslands.  
1180 *Global Change Biology*, **5**, 213-223.
- 1181 Riedo, M., D. Gyalistras, A. Grub, M. Rosset, and J. Fuhrer, 1997: Modelling grassland responses to  
1182 climate change and elevated CO<sub>2</sub>. *Acta Oecologica Applicata*, **18**, 305-311.
- 1183 Rohrer, M. B., 1989: Determination of the transition air temperature and intensity of precipitation.  
1184 Instruments and Observing Methods Report No. 48, 475-482 pp.
- 1185 ———, 1992: Die Schneedecke im Schweizer Alpenraum und ihre Modellierung. Analyse langjähriger  
1186 Schneemessungen und Modellierung des Wasseräquivalentes aufgrund zeitlich hoch aufgelöster  
1187 operationell gemessener meteorologischer Daten. (The snow cover of the Swiss Alps and its  
1188 modelling. Analysis of long-term measurements and modelling of the water equivalent based on  
1189 temporally highly resolved, operationally measured meteorological data.). Zürcher Geographische  
1190 Schriften, 178 pp.
- 1191 Rohrer, M. B., L. N. Braun, and H. Lang, 1994: Long-term records of snow cover water equivalent in the  
1192 Swiss Alps: 1. Analysis. *Nordic Hydrology*, **25**, 53-64.

- 1193 Scherrer, S. C., Appenzeller, C. & Laternser, M. (2004). Trends in Swiss Alpine snow days: The role of  
1194 local- and large-scale climate variability. *Geophys. Res. Lett.*, **31**, L13215,  
1195 doi:10.1029/2004GL020255.
- 1196 Schulla, J., 1997: Hydrologische Modellierung von Flussgebieten zur Abschätzung der Folgen von  
1197 Klimaänderungen (Hydrological modelling of river basins for the assessment of climate change  
1198 impacts). Zürcher Geographische Schriften, 187 pp.
- 1199 Scott, D., Jones, B., Lemieux, C., McBoyle, G., Mills, B., Svenson, S. & Wall, G., 2002: The  
1200 vulnerability of winter recreation to climate change in Ontario's Lakelands Tourism Region.  
1201 Occasional Paper 18, Department of Geography Publication Series, University of Waterloo,  
1202 Waterloo, Canada, 84 pp.
- 1203 Scott, D., G. McBoyle, and B. Mills, 2003: Climate change and the skiing industry in southern Ontario  
1204 (Canada): exploring the importance of snowmaking as a technical adaptation. *Climate Research*, **23**,  
1205 171-181.
- 1206 Seidel, K., Ehrler, C. & Martinec, J., 1998. Effects of climate change on water resources and runoff in an  
1207 Alpine basin. *Hydrol. Processes*, **12**, 1659-1669.
- 1208 Semádeni-Davies, A., 1997: Monthly snowmelt modelling for large-scale climate change studies using the  
1209 degree day approach. *Ecological Modelling*, **101**, 303-323.
- 1210 Semenov, M. A., R. J. Brooks, E. M. Barrow, and C. W. Richardson, 1998: Comparison of the WGEN  
1211 and LARS-WG stochastic weather generators for diverse climates. *Climate Research*, **10**, 95-107.
- 1212 Sevruk, B. 1985: Systematischer Niederschlagsmessfehler in der Schweiz. In: Sevruk, B. (ed) Der  
1213 Niederschlag in der Schweiz. Beitr. Geol. Schweiz. Hydrol. **31**, 65-75.
- 1214 Stadler, D., M. Bründl, M. Schneebeli, M. Meyer-Grass, and H. Flühler, 1998: *Hydrologische Prozesse im*  
1215 *subalpinen Wald im Winter (Hydrological processes in the subalpine forest during wintertime)*.  
1216 vdf Hochschulverlag an der ETH, 145 pp.
- 1217 Trenberth, K. E. and D. A. Paolino Jr., 1980: The Northern Hemisphere sea-level pressure data set: Trends,  
1218 errors and discontinuities. *Monthly Weather Review*, **108**, 855-872.
- 1219 von Storch, H., 1995: Inconsistencies at the interface of climate impact studies and global climate research.  
1220 *Meteorologische Zeitschrift*, **4**, 72-80.
- 1221 von Storch, J.-S., V. Kharin, U. Cubasch, G. Hegerl, D. Schriever, H. von Storch, and E. Zorita, 1997: A  
1222 description of a 1260-year control integration with the coupled ECHAM1/LSG general circulation  
1223 model. *Journal of Climate*, **10**, 1525-1543.
- 1224 von Storch, H. and F. W. Zwiers, 1999: Statistical analysis in climate research. Cambridge University  
1225 Press, 484.
- 1226 von Storch, H., 1999: On the use of inflation in statistical downscaling. *Journal of Climate*, **12**, 3505-  
1227 3506.
- 1228 Wanner, H., D. Gyalistras, J. Luterbacher, R. Rickli, E. Salvisberg, and C. Schmutz, 2000: *Klimawandel*  
1229 *im Schweizer Alpenraum (Climate change in the Swiss Alps)*. vdf, Hochschulverlag AG an der ETH  
1230 Zürich, 285 pp.
- 1231 Whetton, P. H., M. R. Haylock, and R. Galloway, 1996: Climate change and snow-cover duration in the  
1232 Australian Alps. *Climatic Change*, **32**, 447-479.
- 1233 Widmann, M. and C. S. Bretherton, 2000: Validation of mesoscale precipitation in the NCEP reanalysis  
1234 using a new gridpoint data set for the northwestern US. *Journal of Climate*, **13**, 1936-1950.
- 1235 Wielke, L.-M., Haimberger, L. & Hantel, M., 2004: Snow cover duration in Switzerland compared to  
1236 Austria. *Meteorol. Z.*, **13**, 13-17.
- 1237 Witmer, U., 1986: Erfassung, Bearbeitung und Kartierung von Schneedaten in der Schweiz (Registration,  
1238 processing and mapping of snow data in Switzerland). Geographica Bernensia, Series G (Basic  
1239 Research) 3-906290-28-X, 215 pp.
- 1240 WMO, 1986: Intercomparison of models of snowmelt runoff. Operational hydrology report No. 23 92-63-  
1241 10646-0, xxxii + 440 pp.
- 1242